




ORIGINAL RESEARCH

Open Access



Biotic and physical drivers of fire in northwestern Patagonia

Iván Barberá^{1*} , Ana María Cingolani², Florencia Tiribelli³, Mónica Alicia Mermoz⁴, Juan Manuel Morales^{1,5} and Thomas Kitzberger¹

Abstract

Background Understanding the drivers of fire is frequently challenging because some of them interact and influence each other. In particular, vegetation type is a strong control of fire activity, but at the same time it responds to physical and human factors that also affect fire, so their effects are often confounded. We developed a 30 m resolution record of fire for northwestern Patagonia spanning 24 years (July 1998 - June 2022), and present an updated description of fire patterns and drivers. We analysed interannual variation in fire activity in relation to interannual climatic variation, and assessed how topography, precipitation, and human factors determine spatial patterns of fire either directly or by affecting the distribution of vegetation types along physical and human-influence gradients.

Results We mapped 234 fires ≥ 10 ha that occurred between 1999 and 2022, which burned 5.77% of the burnable area. Both the annual burned area and the number of fires increased in warm and dry years. Spatially, burn probability decreased with elevation and increased with slope steepness, irrespective of vegetation type. Precipitation decreased burn probability, but this effect was evident only across vegetation types, not within them. Controlling for physical drivers, forests showed the lowest burn probability, and shrublands, the highest.

Conclusions Interannual climatic variation strongly controls fire activity in northwestern Patagonia, which is higher in warmer and drier years. The climatic effect is also evident across space, with fire occurring mostly in areas of low elevation (high temperature) and low to intermediate precipitation. Spatially, the effect of topography on fire activity results from how it affects fuel conditions, and not from its effect on the distribution of vegetation types. Conversely, the effect of precipitation resulted mostly from the occurrence of vegetation types with contrasting fuel properties along the precipitation gradient: vegetation types with higher fine fuel amount and continuity and intrinsically lower fuel moisture occurred at low and intermediate precipitation. By quantifying the variation in burn probability among vegetation types while controlling for physical factors, we identified which vegetation types are intrinsically more or less flammable. This may help inform fuel management guidelines.

Keywords Correlated drivers, Climate, Topography, Vegetation type, Burn probability

*Correspondence:

Iván Barberá
ivanbarbera93@gmail.com

Full list of author information is available at the end of the article

Resumen

Antecedentes Entender los factores que controlan el fuego resulta desafiante, dado que algunos de ellos interactúan y se influyen entre sí. Particularmente, el tipo de vegetación es un fuerte control de la incidencia del fuego, pero al mismo tiempo responde a factores físicos y humanos que también afectan al fuego, de manera que sus efectos frecuentemente se confunden. Desarrollamos un registro de incendios con una resolución de 30 m abarcando 24 años (julio de 1998 - junio 2022), y presentamos una descripción actualizada de los patrones y controles de estos incendios. Analizamos la variación interanual en la incidencia del fuego y evaluamos cómo la topografía, la precipitación y los factores humanos determinan los patrones espaciales en la ocurrencia de incendios de manera directa o mediante sus efectos sobre la distribución de los tipos de vegetación en un gradiente tanto físico como afectado por la actividad humana.

Resultados Mapeamos 234 incendios ≥ 10 ha que ocurrieron entre 1999 y 2022, y que quemaron 5.77 % del área quemable. Tanto el área quemada como el número de incendios fueron mayores en años cálidos y secos. Espacialmente, la probabilidad de quema disminuyó con la altitud, y aumentó con la pendiente, independientemente del tipo de vegetación. La precipitación disminuyó la probabilidad de quema, aunque este efecto fue evidente sólo entre tipos de vegetación y no dentro de un mismo tipo de vegetación. Al controlar por factores físicos, los bosques mostraron la menor probabilidad de quema, y los matorrales, la mayor probabilidad.

Conclusiones La variación climática interanual controla fuertemente la incidencia del fuego en el noroeste de la Patagonia, la cual es mayor en años cálidos y secos. El efecto climático es también evidente en el espacio, con los incendios ocurriendo en áreas de baja altitud (alta temperatura) y precipitación baja a intermedia. Espacialmente, el efecto de la topografía en la ocurrencia del fuego resulta de su efecto sobre las condiciones del combustible, y no de su control sobre la distribución de los tipos de vegetación. De manera contraria, el efecto de la precipitación resulta en su mayor parte de la ocurrencia de tipos de vegetación con propiedades combustibles contrastantes en el gradiente de precipitación: los tipos de vegetación con gran cantidad y continuidad de combustibles finos e intrínsecamente más baja humedad ocurren en lugares con precipitación baja a moderada. Controlando el efecto de factores físicos, identificamos qué tipos de vegetación son intrínsecamente más o menos inflamables. Esto puede contribuir a informar estrategias de manejo.

Background

Climate change is increasing fire activity in many ecosystems worldwide (Flannigan et al. 2009), emphasizing the need to understand the drivers and mechanisms that influence fire activity (Bowman et al. 2020; Shuman et al. 2022). Two factors are currently limiting our understanding of fire at regional (sub-continental) scales. First, the coarse resolution or low accuracy of systematic, spatially explicit, global fire datasets (Giglio et al. 2018; Long et al. 2019; Lizundia-Loiola et al. 2020) hinders the identification of patterns at higher resolution (Chuvieco et al. 2020). Second, the spatial drivers of fire are frequently correlated, since they influence each other, limiting a more mechanistic understanding of where and why fires occur (Wood et al. 2011). In this context, detailed analyses of fire patterns and drivers based on systematic records of fire at medium resolution (~ 30 m) may help to overcome these limitations. Moreover, the description of fire regimes may serve as a baseline to detect the future changes in fire activity.

Fire activity is strongly determined by climatic conditions and vegetation (fuels). The varying constraints hypothesis proposes that fire activity follows a hump-shaped relationship with productivity: at low

productivity, fire is limited by low fuel amount and horizontal continuity, while at high productivity it is limited mostly by high fuel moisture content (Krawchuk et al. 2009; Krawchuk and Moritz 2011). Hence, intermediate-productivity conditions are proposed to be the most fire-prone (Pausas and Ribeiro 2013). This framework largely explains the temporal and spatial variation in fire activity (e.g., Pricope and Binford 2012; Fischer et al. 2015; Kitzberger et al. 2022).

Temporal variation in fire activity at short temporal scales, ranging from days to a few years, is closely related to climatic variability. In low-productivity systems, fires occur when a rainy or productive period, that allows fuel accumulation, is followed by a dry and or warm period that promotes fuel dessication (Kitzberger et al. 1997; Villagra et al. 2024). In turn, in high-productivity systems, where fuel amount is not a limiting factor, fires occur during dry and or warm periods, when fuel moisture decreases (Sommerfeld et al. 2018; Gaboriau et al. 2022; Cawson et al. 2024). But climate also impacts fire at much longer temporal scales, from centuries to millennia, by affecting vegetation structure and composition, which are tightly linked to productivity (Woodward and McKee 1991;

Box and Fujiwara 2013). Consequently, temporal variations in climate over extended periods may influence fire activity similarly to spatial variations in climate. Thus, insights into the effects of long-term climate can often be inferred from analyses of spatial patterns of fire activity in relation to climate.

The spatial variation of climate generates vegetation variability that is much larger than the variation in fuel amount and moisture observed at short temporal scales. At large spatial scales, the productivity gradient exhibits a wide range of vegetation physiognomies, from deserts to rainforests (Churkina and Running 1998; Chen et al. 2007; Bilgili et al. 2020). At smaller scales, within a more narrow productivity range, vegetation may present sharp changes in composition and structure, defining vegetation types with contrasting flammability (Mitchell et al. 2009). For example, a region of woody vegetation may present tall forests with closed canopy, displaying high vertical fuel discontinuity and a microclimate that promotes high fuel moisture, or short-statured forests and shrublands, with high vertical fuel continuity and lower moisture content (Kitzberger et al. 2016). Hence, spatial climatic variation may affect fire activity in two ways. First, climate may control fuel amount, continuity and moisture, irrespective of vegetation types (e.g., shrublands may be more or less open depending on productivity, but maintaining the shrubland structure). Second, climate may determine the spatial distribution of vegetation types with contrasting flammability. This double effect of climate, and its correlation with vegetation type, hinders the understanding of how vegetation and climate affect fire activity. Interestingly, the same limitation exists for any other fire driver that affects the spatial distribution of vegetation types, as is the case of topography.

In mountain regions, water availability and temperature vary along topographic gradients. Temperature decreases with elevation and towards poleward slopes, thus reducing evapotranspiration (Holden and Jolly 2011; Méndez-Toribio et al. 2016; Jucker et al. 2018; Simon et al. 2024). Water availability is lower in steep slopes compared to plains or valley bottoms, and the latter usually present deeper soils with higher water-holding capacity compared to mid slopes or ridges (Holden and Jolly 2011; Dobrowski 2011; Jucker et al. 2018). Hence, topography, by affecting local climate and soil conditions, may also affect fire activity by controlling the spatial distribution of vegetation types or by affecting fuel amount, continuity and quality within them (Iniguez et al. 2008; Holsinger et al. 2016; Flatley et al. 2011). Moreover, slopes promote the upslope spread of fire and limit it downslope (Rothermel 1983), which is an even more direct effect of topography on fire activity.

Besides these biophysical controls, fire and vegetation are also influenced by human activities. Humans

cause ignitions and suppress fires, but they can also exert an indirect effect by altering vegetation (Bowman et al. 2011; Bar-Massada et al. 2014). In regions of high productivity, forests are frequently logged or burned to promote the growth of grass for cattle raising (Curtis et al. 2018). This shift towards open forests, shrublands or grasslands, despite reducing biomass, may increase the system flammability through a reduction in fuel moisture, an increase in vertical continuity, and an increase in fine fuel density (Pausas and Ribeiro 2013). However, if fuel amount and continuity are significantly reduced, these human-caused transitions may decrease the flammability of the system, instead of increasing it (Blackhall et al. 2017).

Understanding how climate, topography and humans influence the spatial patterns of fire activity, either by shaping vegetation or by more direct effects, requires assessing the effect of these drivers collectively, across and within all vegetation types in the landscape (e.g., Wood et al. 2011). These relationships between fire, vegetation, and fire drivers that affect vegetation may also be evaluated from the vegetation type perspective: the contrasting fire activity among vegetation types may be explained by the physical-human environment where they occur or by their intrinsic fuel properties. Separating the effects of vegetation from the effects of fire drivers that also influence vegetation type is challenging. However, when their association is not so strong, this can be done by comparing fire activity across vegetation types under similar environmental conditions, as well as by comparing the same vegetation type under different environmental conditions.

Fire activity plays an important role in the dynamics of the temperate forests in northwestern Patagonia. These ecosystems, characterized by tree species exhibiting low fire resilience, are susceptible to positive fire-vegetation feedbacks, amplifying their vulnerability to changing environmental conditions (Kitzberger et al. 2012, 2016, 2022). While there is a growing understanding of patterns and drivers of fire activity at landscape and regional scales, most previous studies have been based on non-systematic records of fire (e.g., large, well-documented fires), often performed over smaller administrative units (e.g., specific national parks or other protected areas) and mostly during the late twentieth century (Mermoz et al. 2005; de Torres Curth et al. 2008; Holz et al. 2012; Mundo et al. 2013; Paritsis et al. 2013). Given the strong warming and drying trends in the region there is an urgent need to understand how these conditions are impacting regional fire activity. Only one study analyzed drivers of fire activity during the twenty-first century over a large regional scale, with the aim of predicting future fire activity (Kitzberger et al. 2022). Since the authors focused on

prediction, they did not evaluate how different drivers of fire influence each other, which limits a more mechanistic understanding of spatial controls of fire activity. Moreover, they used mostly coarse-resolution burned area data (MODIS, 500 m), thus hindering the detection of fine scale patterns (e.g., some topographic effects).

In northwestern Patagonia, fire activity is lower in forests than in shrublands (Mermoz et al. 2005; Paritsis et al. 2013; Morales et al. 2015; Tiribelli et al. 2019; Kitzberger et al. 2022). Forests present lower amount of fine fuel, less vertical continuity and moister dead fuels compared to shrublands (Paritsis et al. 2015; Tiribelli et al. 2018; Barberá et al. 2023). However, most forests tend to occur in areas of higher precipitation and elevation compared to shrublands. Under these conditions fuels are expected to be moister compared to areas of lower precipitation and elevation, where shrublands occur. Moreover, shrublands are more abundant near human settlements, where higher fire activity could be explained by higher ignition rate. These patterns suggest that differences in fire activity among vegetation types may be partially explained by the physical and human conditions where they occur, and not only by the differences in fine fuel amount and continuity.

Here we present an updated description of temporal and spatial patterns of fire activity in northwestern Patagonia in the first decades of the twenty-first century, with an emphasis on understanding the effects of correlated fire drivers and how they influence each other. To this end, we developed a systematic record of fire spanning 24 years (July 1998 – June 2022), based on Landsat imagery (30 m resolution). Specifically, we aimed to (1) describe the fire regime in terms of fire size distribution, fire rotation period, and fire seasonality; (2) describe interannual variability in burned area proportion and number of fires in relation to climatic variability; (3) disentangle the role of vegetation and physical and human factors in determining the spatial patterns of fire activity.

Materials and methods

Study area

The study area (2,921,440 ha) encompassed the High Andean and Subantarctic phytogeographic provinces in Argentina, as defined by Oyarzabal et al. (2018; vegetation units 36 and 50), bounded between -39.0° and -44.5° , spanning ~ 600 km in latitude and ~ 70 km in longitude. This region includes nearly all the continuous forests and shrublands in northwestern Patagonia in Argentina (Fig. 1). Non-burnable cover accounts for 25% of the study area according to the vegetation map from Lara et al. (1999), comprising lakes, urban areas, glaciers, and non-vegetated high-andean areas (Fig. 1C). These cover types were excluded from the analyses.

The region presents a sharp precipitation gradient, decreasing from 3000–4000 mm yr^{-1} in the west to ~ 500 mm yr^{-1} in the east (Villalba et al. 2003). The climate is characterized by rainy and snowy winters and dry summers. Mean annual temperature decreases with precipitation and elevation. Elevation ranges from ~ 200 to ~ 3700 m a.s.l., but the burnable area is below ~ 1700 m a.s.l. (Fig. 1), where the mean annual temperature ranges from ~ 0 to 13°C (data from Bianchi and Cravero 2010).

Vegetation varies with elevation, precipitation and local topography (see Appendix 1 for a detailed analysis). Wet forests, dominated by the evergreen tree coihue (*Nothofagus dombeyi* (Mirb.) Oerst.) and the bamboo caña colihue (*Chusquea culeou* E. Desv.), are associated to rainy areas at mid-elevation and low topographic position (e.g., valley bottoms), with intermediate slope steepness. The high-precipitation areas where they occur are usually far from human settlements and roads (Fig. 1C, S1 and S2). Subalpine forests, dominated by the deciduous tree lenga (*Nothofagus pumilio* (Poepp. & Endl.) Krasser), dominate the landscape above ~ 1200 m a.s.l. up to the timberline (1700 m a.s.l.), occupying steep slopes at high topographic position. They occur in areas from intermediate to high precipitation, at intermediate distance from human settlements and roads (Fig. 1C and S1). Dry forests, dominated by ciprés de la cordillera (*Austrocedrus chilensis* (D. Don) Pic.Serm. & Bizzarri), occupy the lowest elevation range at areas of intermediate precipitation, with preference for steep slopes and high topographic position (Fig. 1C, S1 and S2). Shrublands are composed of resprouting short-statured trees or tall shrubs such as ñire (*Nothofagus antarctica* (G. Forst.) Oerst.), caña colihue, radial (*Lomatia hirsuta* (Lam.) Diels ex J.F. Macbr.), laura (*Schinus patagonicus* (Phil.) I.M. Johnst. ex Cabrera) and others. They occur at intermediate elevation and precipitation, mostly at north-facing, gentle slopes (Fig. 1C and S1). Grasslands are represented mostly by the Patagonian steppe, composed mainly of tussock grasses of the genus *Pappostipa* and *Festuca*, and the cushion shrub neneo (*Mulinum spinosum* (Cav.) Pers.). They are the dominant vegetation type at the lowest precipitation range, occurring at gentle slopes in the low to mid elevation range (Fig. 1C and S1). Dry forests, shrublands and grasslands are generally found near human settlements and roads (Fig. S1 and S2). Anthropogenic prairies take place in deforested areas (Fig. 1C) while pine plantations are found at low-elevation and less rugged areas (*Pinus ponderosa* Douglas ex C. Lawson and *Pinus radiata* D. Don).

Fuel amount and continuity vary markedly across vegetation types. Wet and subalpine forests present tall canopies (20–40 m) with high vertical separation from the sparse and moist understory. Conversely, shrublands

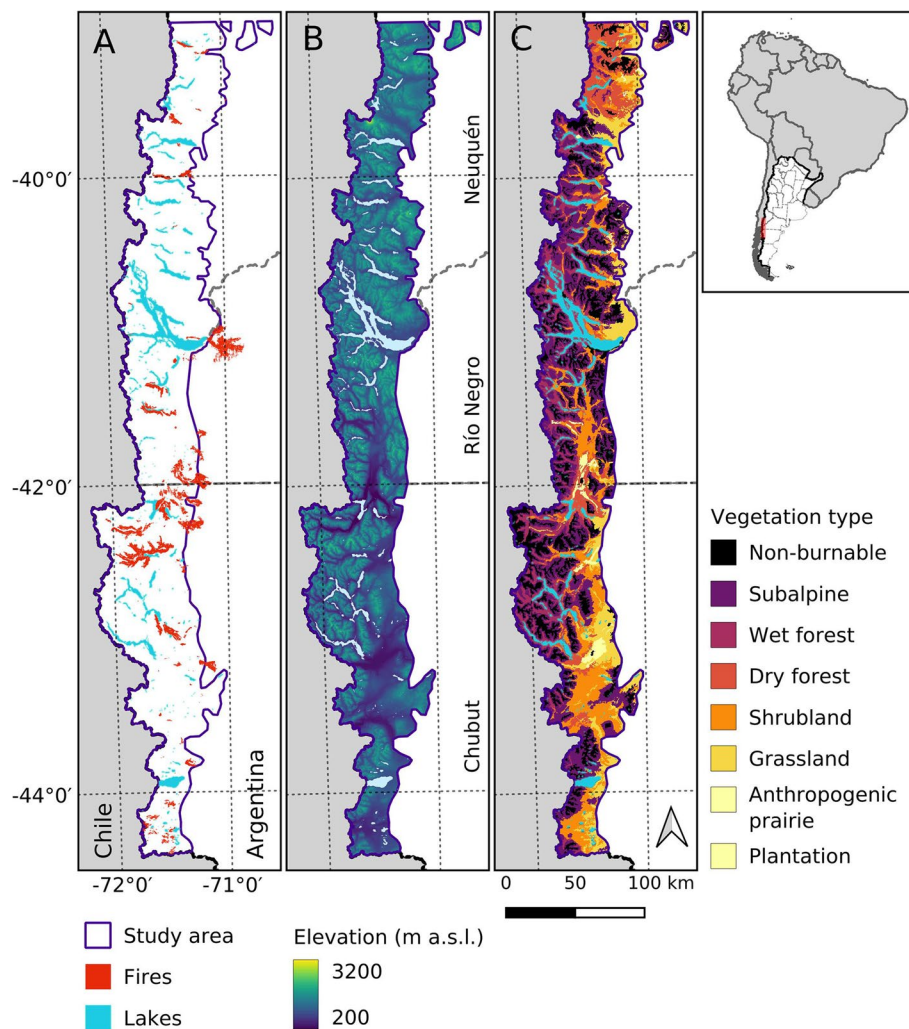


Fig. 1 **A** Map of the study area showing lakes and all fires ≥ 10 ha occurred in 24 years, from July 1998 to June 2022. **B** Elevation and lakes, with labels indicating the Argentinian provinces intersecting the study area. **C** Vegetation types in the study area, modified from Lara et al. (1999)

do not present vertical fuel separation, and have higher proportion of dead fine fuels with lower moisture content compared to forests (Paritsis, et al. 2015; Tiribelli et al. 2018; Barberá et al. 2023). Dry forests are more open than wet and subalpine ones, with more abundance of shrubs and short trees, displaying comparatively higher vertical fuel continuity. Grasslands present low horizontal continuity of fuels, which increases in periods with high precipitation or in areas with high water availability (Kitzberger et al. 1997; Oddi and Ghermandi 2016).

Most fires occur in late spring and summer (October–March), when fuels are dry enough, and ignitions are produced by lightning and by humans (Kitzberger et al. 1997). Although human ignitions are the most frequent cause of fires (82.5%), lightning-started fires

accounted for $\sim 42.7\%$ of burned area in National Parks of northern Patagonia (Bruno and Martin 1982). Lightning, historically rare, is increasing since the late twentieth century (Kitzberger and Veblen 2003; Veblen et al. 2008). The years with highest fire activity are those with warm summers, preceded by dry springs (Kitzberger et al. 2022). These conditions are related to positive anomalies in the Southern Annular Mode and to the alternation of “La Niña-El Niño” phases of El Niño Southern Oscillation during winter-summer, respectively (Kitzberger and Veblen 1997; Holz et al. 2012).

Fires set by humans date from the cultural use of fire by native Americans, occurring mostly at the forest-steppe ecotone (Kitzberger and Veblen 1997). Fire incidence increased at the beginning of the twentieth

century, when Euro-Argentinean settlers burned large extensions of mesic forests to create grasslands in highly productive areas for livestock raising (Kitzberger and Veblen 1997). Since ~1930, fire suppression policies decreased fire activity, but human ignitions are still far more abundant than natural ones (Bruno and Martin 1982; de Torres Curth et al. 2008; Mundo et al. 2013).

Fire mapping

We mapped all fires ≥ 10 ha occurred from July 1998 to June 2022 (24 years; Fig. 1A). The mapping procedure was semi-automatic: first, we produced burned area polygons with an automatic approach using Google Earth Engine (Gorelick et al. 2017), following a similar approach as Long et al. (2019). We used the Normalized Difference Vegetation Index (NDVI) and the Normalized Burn Ratio (NBR), computed from Landsat imagery (30 m resolution). Then we manually edited the fire polygons to amend errors. We retained only polygons ≥ 10 ha, as smaller ones were hard to distinguish from other disturbances. For each fire polygon we obtained the date of occurrence using satellite imagery or records from fire management agencies and news, when available. For well-known fires, we used the date when most of the area was burned, and when this information was not available, we used the mid date between the first and last dates in which fires might have occurred, based on imagery. Using test points identified with Google Earth in and around 22 fires, we estimated a mapping accuracy of 98.06% (Appendix 2.4). Fire mapping methods are fully explained in the supplementary information (Appendix 2). In 1999 few images were available in the study area, so a few fires could not be mapped with desirable precision. To overcome this problem, we included in our database three fires from 1999 mapped by Administración de Parques Nacionales, Argentina (Mermoz 2002).

As most fire activity in our study area occurs between December and March (austral summer), we did not use calendar years, but consider them running from July to June, labelling them with the ending month, for simplicity.

Data analyses

Fire regime: fire rotation period, fire size distribution and fire seasonality

To estimate the fire rotation period across the study area, we counted the number of years in which every burnable pixel (i) burned ($FireCount_i$), averaged this number over all these pixels [$mean(FireCount_i)$] and computed the fire rotation period as $24 \times mean(FireCount_i)^{-1}$, where 24 is the number of years in the study period.

We described the size distribution of all the mapped fires evaluating (1) the cumulative proportion of

burned area as a function of the cumulative number of fires, ordered from the largest to the smallest, and (2) the \log_{10} -frequency of fires as a function of \log_{10} -size classes (Pueyo et al. 2010). For the latter we defined 10 \log_{10} -size classes at 0.5 intervals from 1 to 4.5 (\log_{10} ha), and for each class we computed the average \log_{10} -size of its corresponding fires and the \log_{10} proportion of fires included relative to the total number of fires.

To characterize the fire seasonality (intra-annual variation) we fitted two Generalized Additive Models (GAMs; Wood 2017), using the fire size and the number of fires as response variables. In the fire size model each fire was an observation (232 after removing 2 fires with uncertain date), and in the model for number of fires, observations were month-years (24 years \times 12 months). In both models, we included the month of the year as a continuous predictor (1 to 12 from July to June), and the year as a random effect on the intercept. The month effect was modelled with a cyclic cubic spline of 11 basis functions apart from the intercept ($k=12$ in the *mgcv* R package; Wood 2017). We also present a climate diagram, using mean annual temperature from WorldClim (Hijmans et al. 2005), and mean annual precipitation from the Argentinean Climatic Atlas (Bianchi and Cravero 2010). The climatic data were summarized across the burnable portion of the study area with its mean and percentiles 5 and 95%.

Interannual temporal patterns: fire activity as a function of climatic variation

To explore the effects of interannual climatic variability on fire activity we analysed how the annual burned proportion (burned area over the burnable area) and number of fires ≥ 10 ha (hereafter, number of fires) in the whole study area varied as a function of the climatic variables of the summer period (December–March), averaged across the study area: mean maximum temperature, precipitation, vapour pressure deficit (VPD) and Fire Weather Index, which is a fire danger index computed from precipitation, wind speed, temperature and relative humidity (van Wagner 1987). We obtained monthly precipitation, mean maximum temperature and mean VPD at ~ 4600 m resolution from TerraClimate (Abatzoglou et al. 2018), and daily Fire Weather Index data at $0.25^\circ \times 0.25^\circ$ resolution from the Copernicus Emergency Management Service (Vitolo et al. 2020). TerraClimate data were processed and downloaded using Google Earth Engine (Gorelick et al. 2017), and ClimateEngine was used to download Fire Weather Index data (Huntington et al. 2017). We used the December–March period because most fire activity occurs in these months and because Kitzberger et al. (2022) found it more adequate to predict burn probability compared with longer time

spans. We analysed how the annual burned proportion and number of fires varied as a function of the climatic variables fitting an univariate monotonic GAM for each response and predictor variable. For the burned proportion we applied a \log_{10} transformation to the response and assumed a Normal distribution, and for the number of fires we assumed a Negative Binomial distribution and log link. We did not fit multiple regressions because climatic variables were highly correlated (absolute Pearson's correlation coefficient > 0.65 for most pairs).

We also evaluated whether the burned proportion, number of fires and the climatic variables showed a temporal trend, fitting a Generalized Linear Model (GLM) for each variable with the year as the only predictor. For the annual burned proportion we assumed a Gamma distribution, and for the number of fires, a Negative Binomial, both with log link. For the climatic variables we assumed Normal distribution with identity link. We did not separate human vs. lightning-caused fires, as this information is available only for a small fraction of fires.

Residuals did not show temporal correlation in any model, so we assumed independence between observations.

Spatial patterns: fire activity as a function of biophysical and human factors

To evaluate how biotic, physical, and human factors affect fire activity, we analysed how the probability of a given point in the study area of burning at least once in the study period varied as a function of vegetation type previous to the study period, topography (elevation, slope, aspect and topographic position), precipitation, NDVI, and distance from human settlements and roads, using GAMs. We constructed a 30 m resolution raster stack with all the predictor variables and the response. The burned binary layer (0: non-burned, 1: burned at least once in the study period), was obtained by merging all fire polygons and then rasterizing the result. Vegetation class was obtained from Lara et al. (1999) reclassified as shown in Fig. 1B. Elevation, aspect, slope, and topographic position were obtained from the Shuttle Radar Topography Mission DEM (30 m resolution, Farr et al. 2007), computed in Google Earth Engine (Gorelick et al. 2017). The topographic position was approximated by the pixel elevation scaled between the minimum and maximum values in a 2 km radius. It approaches 0 towards valley bottoms and 1 towards ridges or mountain tops. We defined this variable inspired in Holsinger et al. (2016), who used the difference from mean elevation (Gallant and Wilson 2000), but modified it to avoid over-smoothing in areas with less elevation variation, as the eastern portion of the study area (Fig. 1B). We did not use temperature as predictor because it was highly correlated

with elevation and precipitation (Pearson's $r = -0.67$ and -0.72 , respectively; data from Bianchi and Cravero 2010), but elevation and precipitation were not correlated among them ($r = 0.18$), allowing to estimate separate effects. As a proxy for productivity we used the highest summer-average NDVI (hereafter, NDVI) computed from the whole Landsat imagery between 1999 and 2022 (*NDVI_mean_max* in Appendix 2). Mean annual precipitation was obtained from the Argentinean Climatic Atlas (~ 600 m resolution; Bianchi and Cravero 2010). As proxies for human occupation, we computed the distance to nearest human settlement and to nearest road from Open Street Map (OpenStreetMap Contributors 2015). To fit models of burn probability we sampled points at random from the burnable area with a minimum distance between them of 400 m, yielding 8228 points. From them we extracted the values of the raster stack with all the predictors and the response variable. We did not analyse time since last fire because only 2.58% of the burned area was burned more than once in the study period, and fires occurred before 1999 were documented only for a small fraction of the landscape (analysed in Tiribelli et al. 2019).

To understand how vegetation type and environmental variables (topography, precipitation and distance from human settlements and roads) control fire we compared results from three models of burn probability: (1) a vegetation model, with vegetation type as the only predictor, representing the burn probability of each type under the environmental condition where each occurs (Fig. 6A); (2) an environmental model, including only environmental predictors but not vegetation type, to represent the overall effect of these variables on fire, which represents both their direct effect on fire and also their effect mediated by vegetation type (Figs. 4.1 and 5.1), and (3) a joint model, including the effects of environmental variables, vegetation type, and the vegetation \times environment interaction (Figs. 4.2–6, 5.2–6 and 6C). By comparing predictions from these models we were able to identify how vegetation and environmental factors control fire. Comparing the environmental and joint models allows evaluating whether the effect of a given environmental variable on burn probability is explained by the turnover in vegetation types along its gradient. For example, if the environmental model shows a strong effect of elevation but this effect disappears in the joint model, where vegetation type is included, it is likely that the elevation effect is actually caused by vegetation, and not elevation itself. Similarly, comparing burn probabilities from the vegetation model with those from the joint model, with environmental variables taking the exact same values across vegetation types, allows detecting whether the

environmental conditions where each vegetation type occurs is confounding the effect of intrinsic vegetation properties on fire. For example, if a vegetation type occurs in warm, fire-prone areas, it might show very high burn probability (Fig. 6A); but it could take more moderate values in relation to other types if compared in the same environment (Fig. 6C). Despite separating vegetation vs. environmental effects on fire is challenging, it is feasible with observational data because vegetation types partially overlap along environmental gradients and there is large environmental variation within each type (see Appendix 1).

The three burn probability models were defined as GAMs with Bernoulli response (0: unburned, 1: burned) and logit link function. The effects of environmental variables in the environmental and joint models were modelled with cubic splines of three basis functions ($k=4$ in mgcv), except for aspect, where a cyclic cubic spline was used (Appendix 3.1). In the joint model only the most abundant vegetation types were included (wet forest, subalpine forest, dry forest, shrubland and grassland) to have sufficient data to estimate the effects of environmental variables within each type. In the environmental and joint models we also included the NDVI to help understand the relationships between fire, environmental variables, vegetation type and productivity. However, this predictor was analysed differently from environmental variables, because NDVI is not a causal driver of vegetation type; it rather reflects the vegetation type characteristics.

To compare burn probability across vegetation types under the same environmental conditions (using the joint model) we computed a Partial Dependence Plot (Greenwell 2017) in four partitions of the environmental space: low and high elevation ([500; 900) and [900; 1300) m a.s.l.) combined with low and high precipitation ([750; 1000) and [1000; 1500) mm yr⁻¹; Appendix 3.2). We used two ranges of values for these predictors because they had a large effect on vegetation type, and computing predictions based on their whole distribution in the dataset resulted in unrealistic conditions, where some vegetation types were not likely to occur (*e.g.*, wet forests at low precipitation or subalpine forests at low elevation; Fig. S1). See Appendix 3.2 for details.

To display partial effects of environmental predictors we co-varied their correlated predictors, to avoid creating non-plausible conditions (Appendix 3.3). To summarize the effect of predictors we computed effect sizes for all explanatory variables in all models based on model predictions, quantifying the departure of predicted burn probability from the mean prediction along a partial prediction curve, or across vegetation types (see details

in Appendix 3.4). Effect sizes are shown as percentages inside panels of Figs. 4, 5 and 6.

As spatial correlation leads to an underestimation of uncertainty, instead of computing confidence intervals, we assessed uncertainty by comparing our results to those from randomized fire datasets that exhibited similar correlation. From them, we computed randomized partial predictions and *P*-values (Appendix 3.5).

Software

Data were obtained and prepared using Google Earth Engine (Gorelick et al. 2017), and the analyses were performed in R 4.2.0 (R Core Team 2022). GAMs were fitted with the mgcv package (Wood 2017), and monotonic GAMs, with the scam package (Pya 2024). The data and code to reproduce all analyses and figures are hosted on GitHub (https://github.com/barberaivan/patagonian_fires.git).

Results

Fire regime

During the 24 study years (1999–2022) 234 fires occurred, burning 5.77% of the burnable area (126,594 ha of 2,194,363 ha), with an annual average of 0.25%. Within the burned area, 97.41% burnt only once (123,315 ha), 2.57% burnt twice (3,254 ha), and 0.01% (1,266 ha) burnt three times. The mean fire rotation period was 378 years. The cumulative burned proportion, considering the reburns, was 5.92% (129,906 ha).

The fire size distribution was characterized by a few very large fires and many small ones, with the 24 largest fires (10.08% of the total number of fires) accounting for 78.97% of the cumulative burned area (Fig. 2A). These large fires occurred in 12 of the 24 years. The eight largest fires (3.35% of fires), accounted for nearly half of the burned area (54.14%) and occurred in just four of the 24 years: 1999, 2015, 2021 and 2022. The frequency of fires by size class decreased linearly as a function of fire size when both variables were analysed at the log₁₀ scale (Fig. 2B).

Fire activity was almost zero during winter, increasing to *ca.* one fire by month in spring (October–December) and two fires by month in summer (January–March; Fig. 2C). The average fire size per month did not match the pattern of the number of fires: in spring, fires were relatively small (~200 ha), increasing slightly at the beginning of the summer (January), reaching the largest sizes in February (~1300 ha). In fall (starting in April) both the mean number of fires and mean fire size fell abruptly (Fig. 2C), following the pattern of increasing precipitation (Fig. 2D).

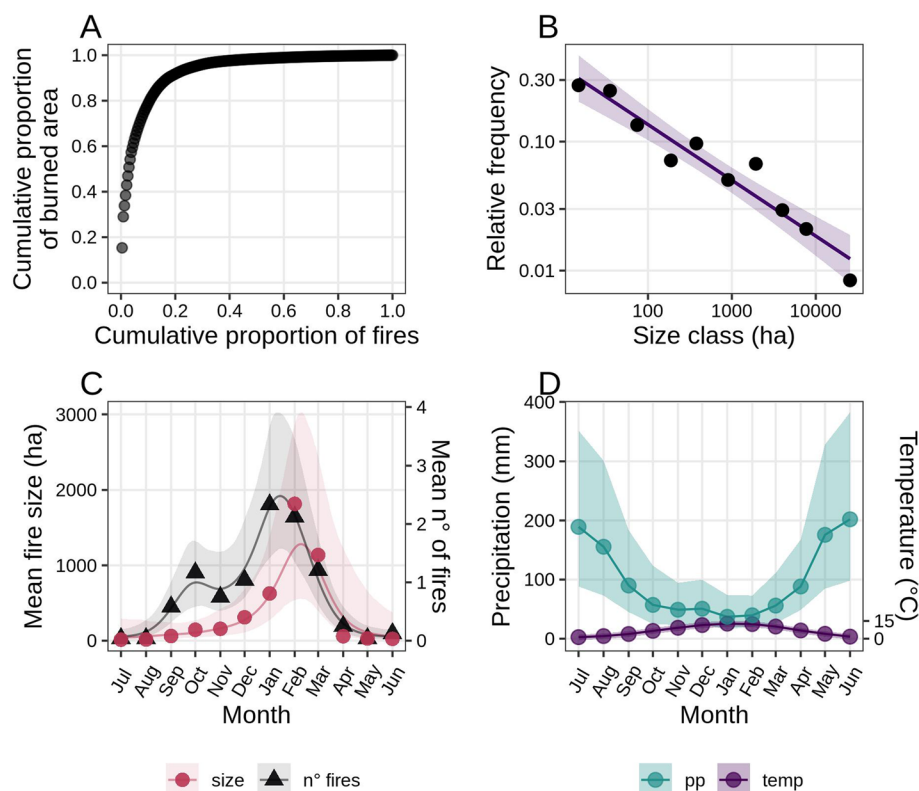


Fig. 2 **A** Cumulative proportion of burned area as a function of the cumulative proportion of fires, ordered from largest to smallest. **B** Relative frequency of fires by size class (both in \log_{10} scale). The line and ribbon show the mean and 95% CI from a linear regression. **C** Mean fire size and number of fires by year and month, averaged over the 24 years. The curves and ribbons show the mean and 95% CI from GAMs, computed for an average year. **D** Mean monthly precipitation and temperature, summarized across the study area with the mean (points) and percentiles 5% and 95% (ribbons). The lines connect points only to improve visibility

Interannual temporal patterns: fire activity as a function of climatic variations

Between 1999 and 2022 the average annual burned proportion relative to the burnable area was 0.25% (5,400 ha), varying mostly between 0.001% (21.24 ha) and 0.78% (17,144 ha), with an extreme value of 2.04% (44,578 ha) in 2015 (Fig. 3A). The annual number of fires varied between 1 and 28, with a mean of 9.92. The annual burned proportion and number of fires showed a slight increasing trend with time, but highly uncertain and with large P -values (0.34 and 0.63, respectively; Table 1). On the contrary, the climatic variables showed clear trends towards dryer and warmer summers, generally with small P -values (Table 1).

The annual burned proportion and number of fires showed a clear variation as a function of climatic variables, with R^2 values ranging from 32 to 60% (Fig. 3B). Both variables increased with temperature, vapour pressure deficit and the fire weather index, and decreased with precipitation (Fig. 3B). The annual burned proportion showed a linear response to temperature, precipitation and Fire Weather Index at the log scale

(implying an exponential response in the original scale), but vapour pressure deficit showed a seemingly saturation effect (Fig. 3B). The number of fires showed a saturation response to all predictors except for the fire weather index, which produced an exponential-like effect (Fig. 3B). However, the saturation effects of vapour pressure deficit on the log-annual burned proportion and the number of fires were highly influenced by the year 2022, which showed the highest vapour pressure deficit, a small number of fires, and moderate burned proportion (Fig. 3).

Spatial patterns: fire activity as a function of biophysical and human factors

In the environmental model, where vegetation type was not considered, elevation and precipitation were the strongest physical controls of burn probability, which was higher in areas of low elevation and precipitation (Figs. 4A.1 and 5A.1). Burn probability also increased towards steep, north-facing slopes, and slightly decreased with topographic position (Fig. 4.1). However, these variables showed smaller effects. NDVI showed a strong

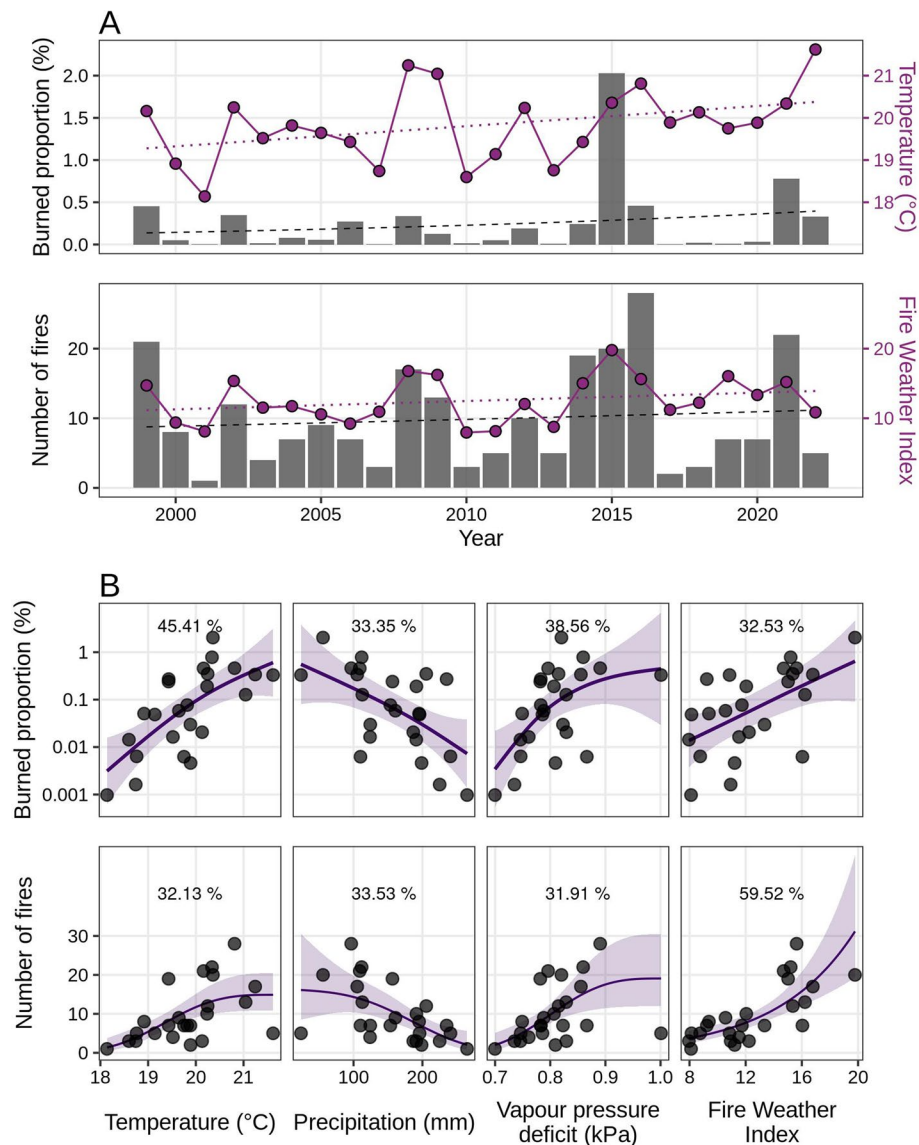


Fig. 3 **A** Annual burned proportion in the landscape (above) and number of fires ≥ 10 ha (below) by year (bars), along with the time series of the climatic variable with strongest effect (temperature and fire weather index, respectively; points and line). Dotted and dashed lines show the predicted mean from the interannual trend models fitted to each variable. **B** Annual burned proportion (above, in log₁₀ scale) and number of fires ≥ 10 ha (below) as a function of climatic variables by year, averaged between December and March. Curves and bands show the fitted means from shape-constrained GAMs with their 95% CI. Numbers inside panels show the Bayesian R^2 (%) (Gelman et al. 2019)

hump-shaped effect, with highest burn probability at intermediate values (Fig. 5B.1). Distance from human settlements and roads largely increased burn probability, but their effects did not depart from chance (Fig. 5D.1).

In the joint model, which allows to predict the effects of environmental variables separately for each vegetation type, the effects of elevation and slope remained qualitatively similar to those from the environmental model, but they varied in magnitude, with the environmental model showing an intermediate effect size in most cases.

In other words, the effects of elevation and slope were maintained within vegetation types, suggesting that they affect fire by themselves, and not due to their association with vegetation type. In wet and dry forests, elevation showed the largest effects on burn probability, but it had considerable uncertainty in the latter ($P=0.386$). In subalpine forests and shrublands elevation showed the smallest effects, not departing from chance ($P=0.776$, Fig. 4A). The positive effect of slope was largest in shrublands, and in grasslands it was negligible (Fig. 4B).

Table 1 Burned proportion, number of fires and climatic variables (averaged over the fire season) as a function of time (year as the only predictor). Burned area and number of fires models were fitted with log link, so $\exp(\beta)$ represents the annual increase factor. The remaining slopes are the annual rates of change at the scale of the response (identity link). Bayesian R^2 values are shown in the last column (Gelman et al. 2019)

Response variable	Slope (β)	SE	t	P	R^2 (%)
Burned proportion (%)	0.046	0.047	0.976	0.340	8.616
Number of fires	0.011	0.022	0.491	0.624	1.032
Temperature (°C)	0.048	0.024	1.992	0.059	14.716
Precipitation (mm)	-3.635	1.658	-2.192	0.039	17.286
Vapour pressure deficit (kPa)	0.006	0.001	3.924	0.001	40.098
Fire Weather Index	0.120	0.094	1.273	0.216	6.582

As opposed to elevation and slope, the effect of aspect was larger in the environmental model than within vegetation types (joint model, Fig. 4C), which means that aspect affects burn probability by controlling the distribution of vegetation types (Fig. S1).

The effect of topographic position was the most variable among vegetation types. It was large and positive in wet and dry forests, but expected from chance ($P=0.258$). In subalpine forests and grasslands, topographic position showed a negligible effect, and in shrublands, a small negative one (Fig. 4D).

Precipitation showed a similar pattern as aspect: the decrease in burn probability with precipitation found in the environmental model blurred in the joint model, where vegetation types were included (Fig. 5A). This means that the effect of precipitation found when vegetation type is not considered results mostly from the turnover of vegetation types along the precipitation gradient (Fig. S1). Within vegetation types, the precipitation effect departed from chance only in subalpine forests, but showing a small effect. And despite in dry forests it showed a larger effect than in the environmental model, it was highly expected by chance. The NDVI showed a hump-shaped effect, which was evident in the environmental model and within most vegetation types in the joint model (Fig. 5B). This effect was largest in wet forests, intermediate in subalpine forests and smaller in grasslands and shrublands. In dry forests the effect of NDVI was large and negative, but was highly expected from chance ($P=0.424$).

Although in the joint model distance from human settlements and roads showed large effects in some vegetation types, in all cases they were highly expected by chance (Fig. 5D), as in the environmental model.

Vegetation types showed clear differences in burn probability in the vegetation model, which did not

include environmental variables (Fig. 6A). Burn probability was higher in dry forests, shrublands and plantations, and lower in subalpine forests and anthropogenic prairies. However, the high and low burn probability of plantations and anthropogenic prairies did not differ from chance. Wet forests and grasslands showed intermediate burn probability (Fig. 6A).

When vegetation types were compared under equal environmental conditions, by using the joint model, they still showed variation in burn probability, but with different patterns compared to those from the vegetation model, and smaller and more uncertain effect sizes (compare Fig. 6A vs. C). This means that burn probabilities estimated by the vegetation model are partly influenced by the contrasting environmental conditions where each vegetation type is more abundant. Although subalpine forests showed the lowest burn probability when environmental variables were not considered (Fig. 6A), they showed values closer to the average when compared at equal conditions. Their burn probability was higher than in wet forests, similar as in grasslands, and lower than in shrublands (Fig. 6C.1 and C.2). Dry forests, with the largest burn probability in the vegetation model, showed lower values than shrublands and similar as grasslands when compared under equal conditions (Fig. 6C.3 and C.4). Wet forests, with an intermediate burn probability in the vegetation model, showed the lowest value when compared at high elevation, and intermediate value at low elevation (Fig. 6C.2 and C.4). Shrubbylands showed the highest burn probability under all conditions, although at low precipitation and elevation, dry forests and grasslands showed similar values (Fig. 6C.3). In addition, their difference from the mean showed larger P-values than in the vegetation model.

The joint model showed the largest explanatory power ($R^2=12.73\%$), followed by the environmental model (8.36%) and the vegetation model (1.51%; Table 2).

Discussion

Fire regime

The annual proportion of burned area, 0.25%, lies within the range reported by previous studies in the region, but is slightly higher: Paritsis et al. (2013) reported 0.08% for the 1984–2010 period, and national parks in our study area report 0.13% for the 1938–1998 period (Bruno and Martin 1982; APN, unpublished data). Although seemingly high, our estimate still lies *ca.* one order of magnitude below burn rates from central Argentina mountain ecosystems (1.3–3.2%; Argañaraz et al. 2020) and from conifer-dominated areas in North America (*e.g.*, 1.7%; Riddle 2023). The relatively low burn rate we found in this *Nothofagus*-dominated area resembles results from broad-leaved forests in the northern hemisphere, which

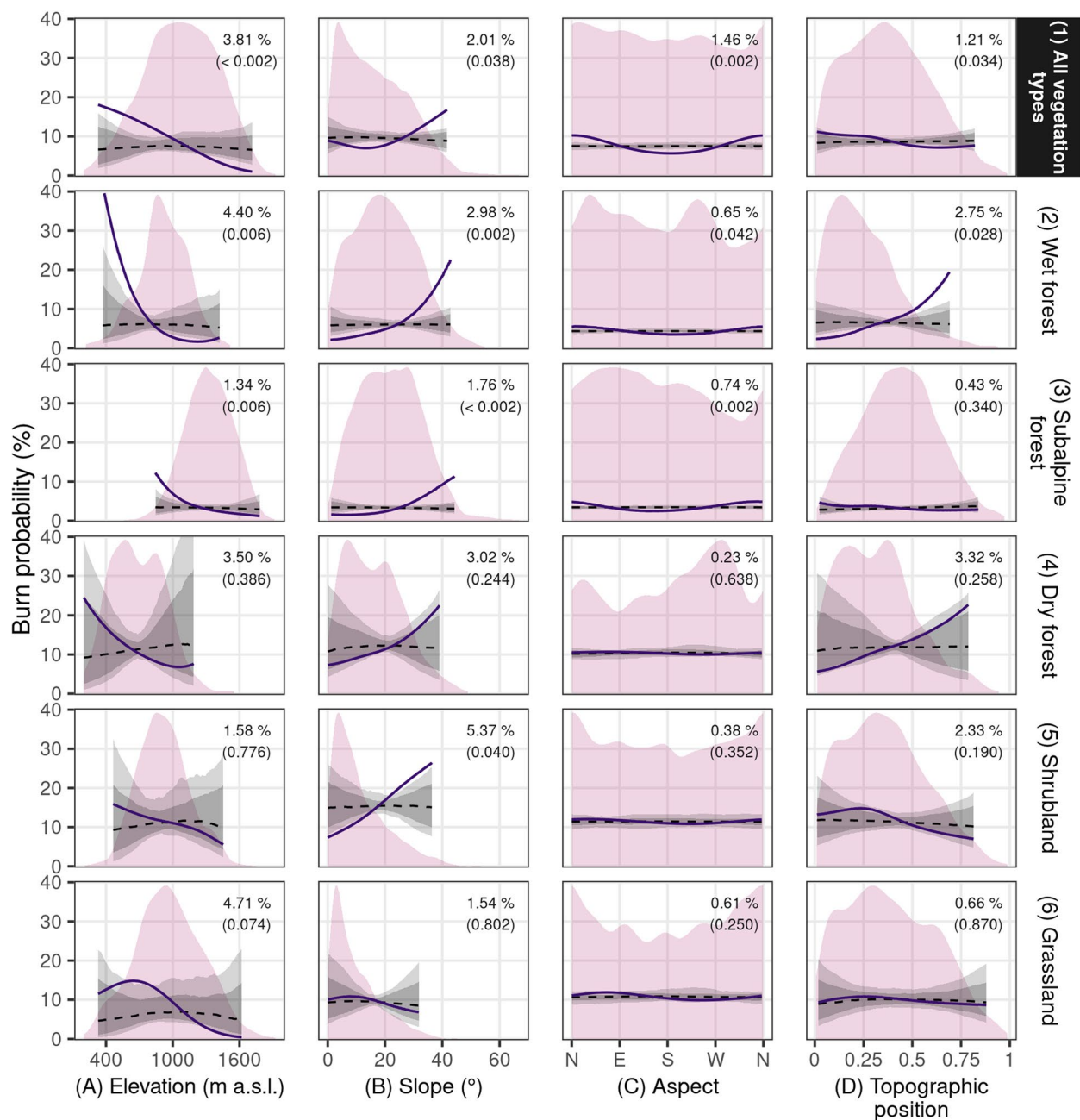


Fig. 4 Burn probability as a function of topographic variables, predicted by the environmental model, where vegetation type was not included (first row), and by the joint model, which includes vegetation types (rows two to six). The solid line shows the prediction from the models fitted to observed data, while the grey ribbons and the dashed line show the distribution of the same prediction made from models fitted to randomized data (median and equal-tailed intervals with 80% and 95% probability). Predictions span the 98% highest density interval of each predictor. The pink shades show the distribution of the predictor variable. Percentages inside panels show the effect size of each predictor, with its corresponding *P*-value

have far lower burn rates than conifer forests (Marchal et al. 2020; Foster et al. 2022).

The intra-annual distribution of fire activity shows that although burned area peaks during the summer (January–March), fires occur since spring, and increase

their frequency in summer. Frequent mid-summer (January and February) fires ignited by humans or lightning can eventually become large because readily burnable fuels (low moisture content) are faced with weather conditions that promote fire spread (maximum number

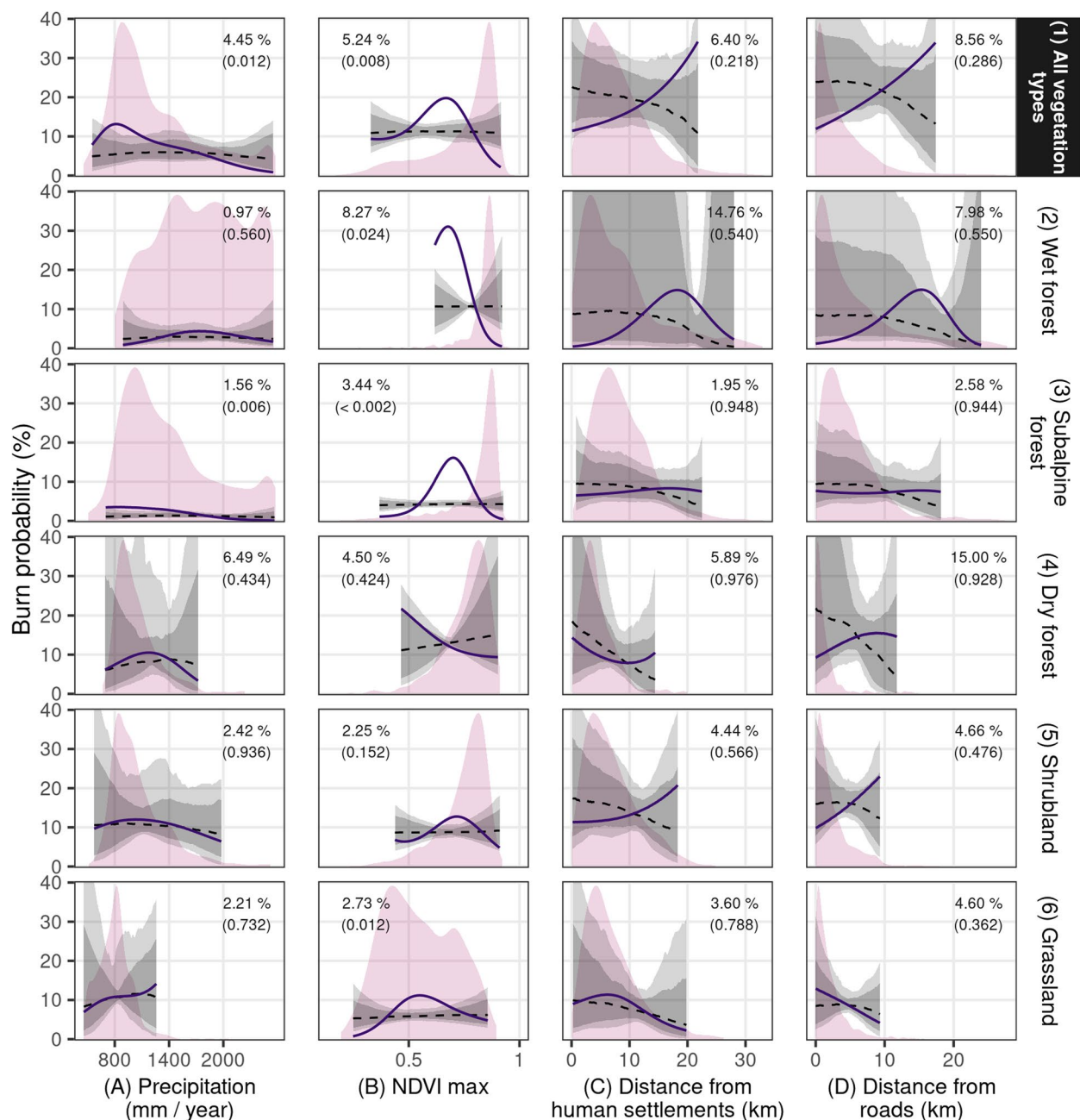


Fig. 5 Burn probability as a function of precipitation, NDVI and distance from human settlements and roads, predicted by the environmental model, where vegetation type was not included (first row), and by the joint model, which includes vegetation types (rows two to six). The solid line shows the prediction from the models fitted to observed data, while the grey ribbons and the dashed line show the distribution of the same prediction made from models fitted to randomized data (median and equal-tailed intervals with 80% and 95% probability). Predictions span the 98% highest density interval of each predictor. The pink shades show the distribution of the predictor variable. Percentages inside panels show the effect size of each predictor, with its corresponding *P*-value

of consecutive days with high temperature, low moisture and or no rain). Spring fires, mostly accidentally ignited by humans, tend to remain small given high vegetation moisture levels and less favourable weather for spreading fires (Barberá et al. 2023). In our study

area, the burned area and number of fires decreased sharply when the autumn begins, despite a high abundance of deciduous species. Apparently, the abundant precipitation in April offsets the effects of fuel drying related to senescence, which contrasts with deciduous

forests with lower precipitation in autumn (e.g., Tian et al. 2011).

Temporal patterns: burned area as a function of interannual climatic variability

Besides the clear seasonal pattern, we also found strong effects of interannual climatic variability on burned area and number of fires, showing that fire activity increases in years with drier and warmer summers (Kitzberger et al. 1997, 2022; Kitzberger and Veblen 1997; Holz et al. 2012; de Torres Curth et al. 2008). Other studies show that this effect increases when drought occurs since the winter prior to the fire season, which suggests a cumulative effect of water deficit on fuel moisture (Kitzberger et al. 1997, 2022; Kitzberger and Veblen 1997; de Torres Curth et al. 2008). The larger burned area during warm and dry summers is clearly explained by fuel moisture, but as lightning activity increases under these conditions, a higher ignition rate may contribute to this pattern (Kitzberger et al. 1997). Interannual climatic variability also largely explains burned area patterns in other boreal and temperate forests (Gaboriau et al. 2022; Gill and Taylor 2009; Seidl et al. 2020; Sommerfeld et al. 2018; Whitlock et al. 2015).

Despite the relatively short record, we found a tenuous increasing trend in burned area and number of fires, similar to the pattern found in a longer time series. Although this trend showed a large P-value, the increase in burned proportion and number of fires agree with a predicted positive phase for the Antarctic Oscillation during the twenty-first century (Thompson et al. 2011), which indicates a change towards more fire-promoting climate, also evident in our climatic time series, with a clear trend towards warmer and dryer summers. In addition, the projected fire probability under global warming scenarios in northwestern Patagonia is expected to increase by a factor from 3 to 8 relative to the current values by the end of the century, depending on the climatic scenario (Kitzberger et al. 2022). Moreover, the climatic effects and trends found in our study match observations around the globe, with higher fire incidence related to climate change (Wang et al. 2015; Robinne et al. 2018; Ellis et al. 2022; Lund et al. 2023). Hence, the high uncertainty in the increasing trend in burned area is likely a result of low statistical power. This trend will probably become statistically clearer

when more years are analysed. In particular, separate analyses of trends in burned area from lightning vs. human-caused fires might help project fire activity, as both causes may respond differently to climate change, and present contrasting challenges for fire management. Lightning activity is expected to increase in northwestern Patagonia with climate change (Veblen et al. 2008), and might account for most of burned area in the future, as reported in other regions (Miller et al. 2012; Cattau et al. 2020).

Spatial patterns: fire activity as a function of biophysical and human factors

Vegetation type and the physical environment affect fire activity, but understanding their influence is challenging because vegetation type varies along environmental gradients. Despite these effects cannot be perfectly isolated with observational data, our study improved the understanding of their separate effects on fire. We found that although topography strongly determines vegetation type in northwestern Patagonia, its largest effects on fire activity cannot be explained by the turnover of vegetation along topographic gradients. Instead, most of its effects are evident within most vegetation types. Conversely, the decrease in fire activity with precipitation and in south-facing slopes is mostly explained by how vegetation types with contrasting fuel amount and continuity vary along the precipitation gradient and between slopes of different aspect.

The marked decrease in burn probability with elevation likely results from a decrease in temperature, hence reducing evapotranspiration and slowing the dessication of fuels. Similarly, the reduction in burn probability in areas with low steepness and located at low topographic position can be explained by the higher water accumulation and lower runoff in those sites. As these conditions promote high fuel moisture, it is expected that similar effects of topography are found in all vegetation types. In addition, steep slopes may burn more than flatter areas because they promote the uphill spread of fire, but do not limit downhill spread as much. This effect is also expected to operate in all vegetation types. Nevertheless, the effects of topography showed some variation among vegetation types. In some cases, this variation is explained by the contrasting weight of other predictors that co-vary

(See figure on next page.)

Fig. 6 **A** Burn probability as a function of vegetation type, predicted by the vegetation model. **B** Relative abundance of each vegetation type in the burnable area. **C** Burn probability as a function of vegetation type, predicted by the joint model at four environmental conditions, as a partitioned Partial Dependence Plot (Appendix 3.2). Vegetation types are missing in environmental conditions where they are unlikely to occur. In **A** and **C**, the dashed horizontal lines show the average burn probability across vegetation types weighted by relative abundance. Numbers above bars show the two-tailed P-values for burn probabilities (Appendix 3.5), and the percentage inside each panel shows the effect size of vegetation type with its corresponding P-value (Appendix 3.4)

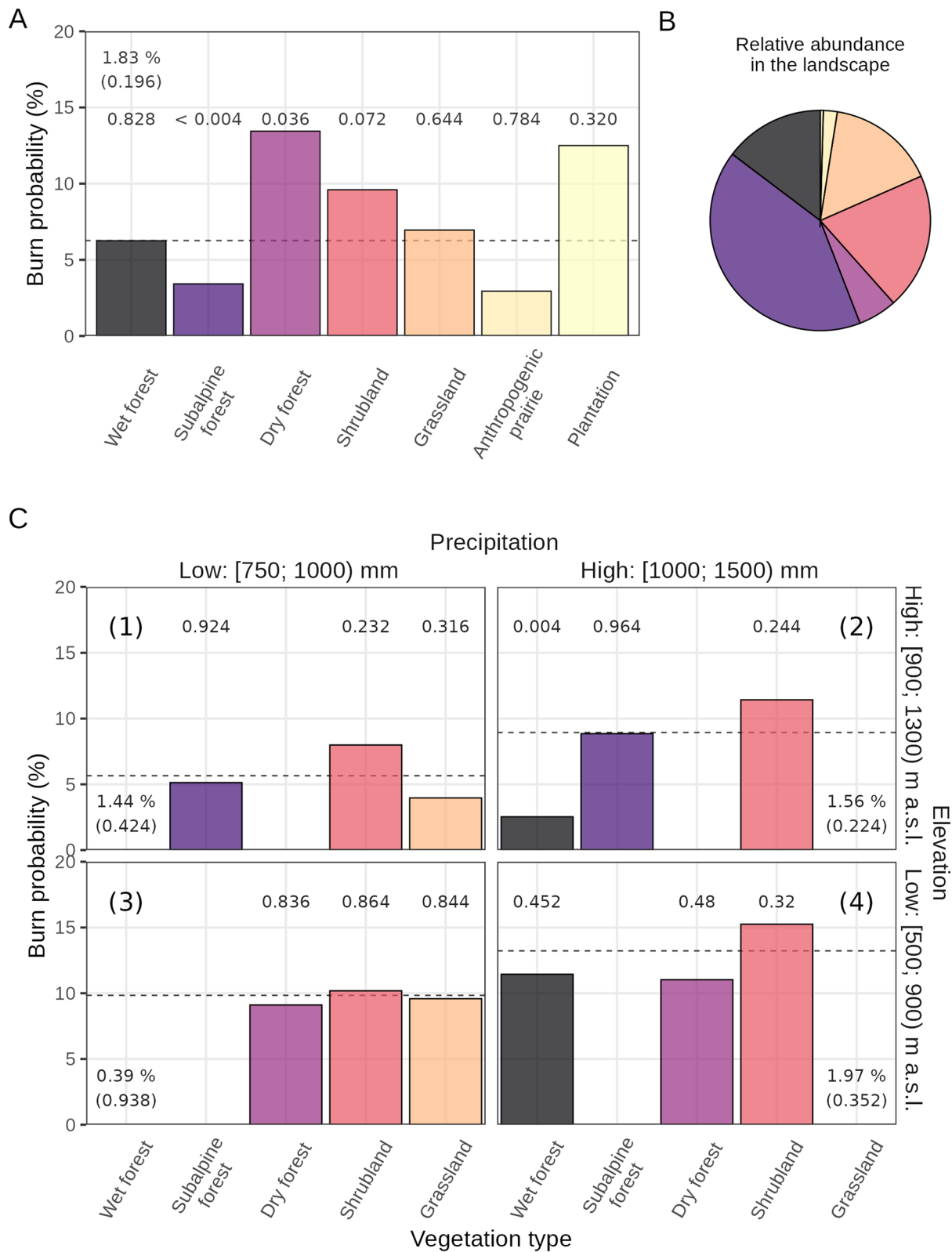


Fig. 6 (See legend on previous page.)

Table 2 Bayesian R^2 (Gelman et al. 2019) for the three burn probability models and metrics of a Likelihood Ratio Test comparing the vegetation and environmental models against the joint model

Model	Bayesian R^2 (%)	Chi squared	Degrees of freedom	P-value
Vegetation	1.51	677.65	67.532	< 2.2E-16
Environmental	8.36	249.01	56.583	< 2.2E-16
Joint	12.73	-	-	-

with elevation but have the opposite effect. For example, in grasslands, slope and topographic position do not affect burn probability because as they increase, elevation increases too, outweighing their effects. But when controlling for elevation, slope and topographic position increase burn probability (Appendix 3.3, Fig. S8). A similar phenomenon explains the relatively low importance of elevation in subalpine forests. As elevation increases, slopes become steeper and NDVI decreases (Fig. S4 and S7A.3), counteracting the effect of lower temperature on burn probability. Again, controlling for slope and NDVI, elevation shows a large effect in subalpine forests (Fig. S8). However, in the case of shrublands, the low importance of elevation is not explained by counteracting effects of other predictors, but likely results from their physiognomy. As they have high fine fuel amount and continuity and a microclimate that promotes fuel dryness (Paritsis et al. 2015; Tiribelli et al. 2018; Barberá et al. 2023), the lower temperature at higher elevation probably cannot reduce as much their flammability. Finally, the large P-values of the elevation effects in dry forests and in shrublands likely result from the low abundance of the former, and the small effect in the latter, which decrease statistical power.

Contrary to the most important topographic controls of fire, the effect of precipitation observed when vegetation types were not considered (in the environmental model), seems to be explained mostly by the turnover of vegetation type along the precipitation gradient (Fig. S1), and not so much by how precipitation affects fuel conditions within vegetation types. The lowest burn probability found at high precipitation areas is likely explained by the high abundance of wet and subalpine forests (Fig. S1), which have low vertical fuel continuity and an understorey with intrinsically high moisture (Paritsis et al. 2015; Tiribelli et al. 2018; Barberá et al. 2023). As precipitation decreases, the increase in shrubland cover seems to increase flammability, as they present higher fuel amount and continuity and lower

fuel moisture related to the lack of a closed canopy. But at the lowest precipitation range, below 800 mm yr⁻¹, precipitation seems to affect fire by its control on fuels within vegetation types. Below 800 mm yr⁻¹, where grasslands are the dominant vegetation type (Fig. S1), burn probability decreases with decreasing precipitation (Fig. 5A.1). Hence, that decrease in burn probability occurs because grasslands present lower productivity at low precipitation (Fig. S7E.6), and fire is limited by fuel continuity.

We found that differences in burn probability among vegetation types are explained both by their contrasting fuel amount and continuity, and by the topographic conditions where each one is more abundant. The low and high burn probability found in subalpine and dry forests, respectively, when the environmental predictors are not considered, is largely explained by their occurring at the highest and lowest elevation ranges. When compared with other vegetation types under equal conditions, dry forests showed relatively low burn probability, and subalpine forests, intermediate values. Subalpine forests were expected to show similar burn probability as wet forests, due to their structural similarity, but instead they showed higher burn probability. This could be explained by *N. pumilio* trees being shorter, which would increase vertical fuel continuity.

Our results agree with the varying constraints hypothesis, with the intermediate productivity areas showing the highest burn probability (Pausas and Ribeiro 2013; Krawchuk and Moritz 2011), in accordance with Kitzberger et al. (2022). This pattern was evident also within vegetation types, and our results suggest that low-productivity wet and subalpine forests could present even higher burn probability than shrublands. These forests with relatively low NDVI (~0.7) are likely those with open canopies, where fuel amount is high and fuel moisture is low. In shrublands, NDVI showed smaller effects on fire activity than in most of the other vegetation types, suggesting that despite presenting variable fuel amount and continuity, they never reach conditions that reduce markedly burn probability, as they rarely present closed, tall canopies.

Contrary to the clear effects of vegetation and topography on fire activity, we found an unclear effect of distance from human settlements and roads. But despite the increase in burn probability at longer distances is highly expected by chance, it could also result from lightning-caused fires, which starting far from human settlements and roads are less likely to be detected and controlled. Studies analysing separately ignitions and spread and accounting for ignition source (lightening vs. human) are necessary to better understand the human effects on fire

(e.g., Mundo et al. 2013; Morales et al. 2015; Godoy et al. 2022).

Our analysis improved the understanding of the separate effects of vegetation and environmental variables on fire, although we acknowledge that this observational approach cannot fully isolate them. Specifically, our results highlighted differences in burn probability among vegetation types which are likely the result of contrasting fuel properties (Fig. 6C) rather than environmental variation. However, we recognize that the observed differences between vegetation types, even when controlling for environmental factors (Fig. 6C), may still be partially influenced by unobserved environmental variables (e.g., soil depth, soil moisture). Overall, our study provides a foundation for more detailed field research to further refine our understanding of vegetation and environmental drivers of fire.

Implications for fire management

In ecosystems where flammability increases with time since fire, as in the Northern Hemisphere conifer forests, low-severity, frequent fires limit the occurrence of extremely large, severe ones (Ryan et al. 2013). However, if (1) flammability is higher in the early seral stages than in the mature ones, or (2) fire-resilient vegetation types are more flammable than fire-sensitive ones, adding fire to the system is expected to promote more fire (Kitzberger et al. 2012; Tiribelli et al. 2019). Northwestern Patagonian vegetation meets both conditions. Forests, the least flammable vegetation types, increase their flammability when vegetation is recovered after fire (Tiribelli et al. 2018, 2019; Barberá et al. 2023), but their post-fire regeneration is limited (Cuevas 2000; Kitzberger et al. 2005; Landesmann and Morales 2018; Tercero-Bucardo et al. 2007). In turn, shrublands, the most flammable vegetation type, persist after fire and frequently replace burned forests (Kitzberger et al. 2016; Landesmann et al. 2021). These dynamics result in frequent fire promoting more flammable vegetation, which in turns promotes more fire. Hence, to reduce the impacts of fire on society and ecosystems, which are expected to increase with climate change, it is necessary to limit fire activity as much as possible.

We found that the most productive woody communities tend to burn less. Despite the low burn probability found at high NDVI areas may result from high water availability related to small-scale physical conditions (e.g., high soil moisture, less insolation), this may also reflect a particular vegetation structure. High productivity areas usually present tall, closed canopies, which produce low-biomass understoreys, with low vertical fuel continuity, and or high fuel moisture. Hence, promoting the growth of tall trees to create closed

canopies that increase fuel moisture and reducing fuel amount and continuity in the understoreys could reduce flammability significantly. Tall, closed canopies can be induced with shrubland management practices, such as pruning short, multi-stemmed trees (such as *radal* or *ñire*) to make them single-stemmed and promote vertical growth, or planting *coihue*, *lenga* and *ciprés* trees in the shrubland matrix. Understorey fuels could be reduced by combining firewood and timber extraction with livestock raising, which show promising economic value (Peri et al. 2016; Goldenberg et al. 2018, 2021). However, as fine fuel moisture may also be decreased by harvesting, careful strategies are needed to effectively decrease flammability (Goldenberg et al. 2020). But future climate is expected to generate fire that will probably spread even through this less-flammable settings (Cawson et al. 2024), casting doubts on these fuel management as the only strategy. Thus, reducing human ignitions and generating more effective early fire and ignition detection systems could be the most effective strategy to reduce fire vulnerability across this region. Finally, predictions from fire spread models may help during the suppression process. This study points out directions to improve the performance of fire spread models recently developed in the region (Morales et al. 2015; Laneri et al. 2020), by including variables such as elevation, NDVI and vegetation type.

Conclusions

Our results confirm the strong effect of interannual climatic variation on fire activity in northwestern Patagonia, and also suggest that climate change will increase fire activity, in accordance with previous research (Kitzberger et al. 2022). Spatially, we found that the effect of topography on fire activity cannot be explained by the turnover in vegetation types along topographic gradients. Instead, topography is probably affecting fire mostly through its effect on water balance and hence, fuel moisture content, with a similar effect across vegetation types. Conversely, the effect of mean annual precipitation on fire activity is explained by the occurrence of vegetation types with contrasting fine fuel amount, continuity and moisture along the gradient.

Our description of burned area patterns for the beginning of the twenty-first century may serve as a reference point to detect changes in fire regime in the region, and our fire mapping algorithm may be used to keep this record up to date. Moreover, a better understanding of how fire responds to biophysical and human factors could be achieved by studying separately fire ignition and spread, for which our results and database provide a valuable starting point.

Supplementary Information

The online version contains supplementary material available at <https://doi.org/10.1186/s42408-025-00353-8>.

Supplementary Material 1.

Acknowledgements

Administración de Parques Nacionales (Argentina) provided a few fire polygons. We thank the editor Stacy Drury and two anonymous reviewers who helped improve this manuscript.

Authors' contributions

IB, FT, AC and TK conceived the idea. IB collected and analysed the data and wrote the first version of the manuscript. MM provided additional data. TK, AC, FT, MM and JMM revised and edited the manuscript.

Funding

This study was funded by Ministerio de Ciencia, Tecnología e Innovación Productiva (Argentina), Agencia Nacional de Promoción de la Investigación, el Desarrollo Tecnológico y la Innovación, grant PICT-2017–2142. Iván Barberá received a PhD scholarship from Consejo Nacional de Investigaciones Científicas y Tecnológicas (Argentina).

Data availability

The data and code to reproduce all analyses and figures are hosted on GitHub (https://github.com/barberaivan/patagonian_fires.git).

Declarations

Ethics approval and consent to participate

Not applicable.

Consent for publication

Not applicable.

Competing interests

The authors declare that they have no competing interests.

Author details

¹Instituto de Investigaciones en Biodiversidad y Medioambiente, CONICET – Universidad Nacional del Comahue, Bariloche 8400, Argentina. ²Instituto Multidisciplinario de Biología Vegetal, CONICET – Universidad Nacional de Córdoba, Córdoba 5000, Argentina. ³Department of Forest and Conservation Sciences, Faculty of Forestry, University of British Columbia, Vancouver V6T 1Z4, Canada. ⁴Formerly at Delegación Regional Patagonia, Administración de Parques Nacionales, Bariloche 8400, Argentina. ⁵School of Biodiversity, One Health and Veterinary Medicine, University of Glasgow, Glasgow G12 8QQ, UK.

Received: 1 May 2024 Accepted: 27 January 2025

Published online: 13 March 2025

References

- Abatzoglou, J.T., T. Solomon, Z. Dobrowski, S.A. Parks, and K.C. Hegewisch. 2018. TerraClimate, a high-resolution global dataset of monthly climate and climatic water balance from 1958–2015. *Scientific Data* 5 (1): 1–12. <https://doi.org/10.1038/sdata.2017.191>.
- Argañaraz, J.P., A.M. Cingolani, L.M. Bellis, and M.A. Giorgis. 2020. Incidencia del fuego en un gradiente altitudinal de las sierras del centro de la Argentina. *Ecología Austral* 30 (2): 268–81. <https://doi.org/10.25260/EA.20.30.2.0.1054>.
- Barberá, I., J. Paritsis, L. Ammassari, J.M. Morales, and T. Kitzberger. 2023. Microclimate and species composition shape the contribution of fuel moisture to positive fire-vegetation feedbacks. *Agricultural and Forest Meteorology* 330: 109289. <https://doi.org/10.1016/j.agrformet.2022.109289>.
- Bar-Massada, A., V.C. Radeloff, and S.I. Stewart. 2014. Biotic and abiotic effects of human settlements in the wildland–urban interface. *BioScience* 64 (5): 429–437. <https://doi.org/10.1093/biosci/biu039>.
- Bianchi, A.R., and S.A.C. Cravero. 2010. Atlas climático digital de la República Argentina. Ediciones INTA; Estación Experimental Agropecuaria Salta. https://www.argentina.gob.ar/sites/default/files/inta-atlas_climatico_digital_argentina-2010.pdf.
- Bilgili, B.C., S. Erşahin, S.S. Kavaklıgil, and N. Öner. 2020. Net primary productivity of a mountain forest ecosystem as affected by climate and topography. *Cerne* 26: 356–368. <https://doi.org/10.1590/01047760202026032730>.
- Blackhall, M., E. Raffaele, J. Paritsis, F. Tiribelli, J.M. Morales, T. Kitzberger, J.H. Gowda, and T.T. Veblen. 2017. Effects of biological legacies and herbivory on fuels and flammability traits: a long-term experimental study of alternative stable states. *Journal of Ecology* 105 (5): 1309–1322. <https://doi.org/10.1111/1365-2745.12796>.
- Bowman, D.M.J.S., J. Balch, P. Artaxo, W.J. Bond, M.A. Cochrane, C.M. D'antonio, R. DeFries, et al. 2011. The human dimension of fire regimes on Earth. *Journal of Biogeography* 38 (12): 2223–2236. <https://doi.org/10.1111/j.1365-2699.2011.02595.x>.
- Bowman, D.M.J.S., C.A. Kolden, J.T. Abatzoglou, F.H. Johnston, G.R. van der Werf, and M. Flannigan. 2020. Vegetation fires in the Anthropocene. *Nature Reviews Earth & Environment* 1 (10): 500–515. <https://doi.org/10.1038/s43017-020-0085-3>.
- Box, E.O., and K. Fujiwara. 2013. Vegetation types and their broad-scale distribution. *Vegetation Ecology*, 455–85. <https://doi.org/10.1002/9781118452592.ch15>.
- Bruno, J., and C. Martin. 1982. Los incendios forestales en los Parques Nacionales: Estudio estadístico y análisis de incidencia, Administración de Parques Nacionales, 45. Buenos Aires: Administración de Parques Nacionales.
- Cattau, M.E., C. Wessman, A. Mahood, and J.K. Balch. 2020. Anthropogenic and lightning-started fires are becoming larger and more frequent over a longer season length in the USA. *Global Ecology and Biogeography* 29 (4): 668–681. <https://doi.org/10.1111/geb.13058>.
- Cawson, J.G., L. Collins, S.A. Parks, R.H. Nolan, and T.D. Penman. 2024. Atmospheric dryness removes barriers to the development of large forest fires. *Agricultural and Forest Meteorology* 350: 109990. <https://doi.org/10.1016/j.agrformet.2024.109990>.
- Chen, X.F., J.M. Chen, S.Q. An, and W.M. Ju. 2007. Effects of topography on simulated net primary productivity at landscape scale. *Journal of Environmental Management* 85 (3): 585–596. <https://doi.org/10.1016/j.jenvman.2006.04.026>.
- Churkina, G., and S.W. Running. 1998. Contrasting climatic controls on the estimated productivity of global terrestrial biomes. *Ecosystems* 1: 206–215. <https://doi.org/10.1007/s100219900016>.
- Chuvieco, E., I. Aguado, J. Salas, M. García, M. Yebra, and P. Oliva. 2020. Satellite remote sensing contributions to wildland fire science and management. *Current Forestry Reports* 6: 81–96. <https://doi.org/10.1007/s40725-020-00116-5>.
- Cuevas, J.G. 2000. Tree recruitment at the *Nothofagus pumilio* alpine timberline in Tierra del Fuego, Chile. *Journal of Ecology* 88 (5): 840–855. <https://doi.org/10.1046/j.1365-2745.2000.00497.x>.
- Curtis, P.G., C.M. Slay, N.L. Harris, A. Tyukavina, and M.C. Hansen. 2018. Classifying drivers of global forest loss. *Science* 361 (6407): 1108–1111. <https://doi.org/10.1126/science.aau3445>.
- Dobrowski, S.Z. 2011. A climatic basis for microrefugia: The influence of terrain on climate. *Global Change Biology* 17 (2): 1022–1035. <https://doi.org/10.1111/j.1365-2486.2010.02263.x>.
- Ellis, T.M., D.M.J.S. Bowman, P. Jain, M.D. Flannigan, and G.J. Williamson. 2022. Global increase in wildfire risk due to climate-driven declines in fuel moisture. *Global Change Biology* 28 (4): 1544–1559. <https://doi.org/10.1111/gcb.16006>.
- Farr, T.G., P.A. Rosen, E. Caro, R. Crippen, R. Duren, S. Hensley, M. Kobrick, et al. 2007. The shuttle radar topography mission. *Reviews of Geophysics* 45: 1–13. <https://doi.org/10.1029/2004RG000410>.
- Fischer, M.A., C.M. Di Bella, and E.G. Jobbágy. 2015. Influence of fuel conditions on the occurrence, propagation and duration of wildland fires: a regional approach. *Journal of Arid Environments* 120: 63–71. <https://doi.org/10.1016/j.jaridenv.2015.04.007>.

- Flannigan, M.D., M.A. Krawchuk, W.J. de Groot, B.M. Wotton, and L.M. Gowman. 2009. Implications of changing climate for global wildland fire. *International Journal of Wildland Fire* 18 (5): 483–507. <https://doi.org/10.1071/WF08187>.
- Flatley, W.T., C.W. Lafon, and H.D. Grissino-Mayer. 2011. Climatic and topographic controls on patterns of fire in the southern and central Appalachian Mountains, USA. *Landscape Ecology* 26: 195–209. <https://doi.org/10.1007/s10980-010-9553-3>.
- Foster, A.C., J.K. Shuman, B.M. Rogers, X.J. Walker, M.C. Mack, L.L. Bourgeau-Chavez, S. Veraverbeke, and S.J. Goetz. 2022. Bottom-up drivers of future fire regimes in western boreal North America. *Environmental Research Letters* 17 (2): 025006. <https://doi.org/10.1088/1748-9326/ac4c1e>.
- Gaboriau, D.M., H. Asselin, A.A. Ali, C. Hély, and M.P. Girardin. 2022. Drivers of extreme wildfire years in the 1965–2019 fire regime of the Tłı̨chǫ First Nation Territory. *Canada. Ecoscience* 29 (3): 249–265. <https://doi.org/10.1080/11956860.2022.2070342>.
- Gallant, J.C., and J.P. Wilson. 2000. Primary topographic attributes. In *Terrain Analysis: Principles and Applications*, ed. J. Wilson and J. Gallant, 51–85. New York: Wiley.
- Gelman, A., B. Goodrich, J. Gabry, and A. Vehtari. 2019. R-squared for Bayesian regression models. *The American Statistician*. <https://doi.org/10.1080/00031305.2018.1549100>.
- Giglio, L., L. Boschetti, D.P. Roy, M.L. Humber, and C.O. Justice. 2018. The Collection 6 MODIS burned area mapping algorithm and product. *Remote Sensing of Environment* 217: 72–85. <https://doi.org/10.1016/j.rse.2018.08.005>.
- Gill, L., and A.H. Taylor. 2009. Top-down and bottom-up controls on fire regimes along an elevational gradient on the east slope of the Sierra Nevada, California, USA. *Fire Ecology* 5: 57–75. <https://doi.org/10.4996/fireecology.0503057>.
- Godoy, M.M., S. Martinuzzi, P. Masera, and G.E. Defossé. 2022. Forty years of wildland urban interface growth and its relation with wildfires in central-western Chubut, Argentina. *Frontiers in Forests and Global Change* 5: 850543. <https://doi.org/10.3389/ffgc.2022.850543>.
- Goldenberg, M.G., J.H. Gowda, C. Casas, and L.A. Garibaldi. 2018. Efecto de la tasa de descuento sobre la priorización de alternativas de manejo del matorral norpatagónico argentino. *Bosque (Valdivia)* 39 (2): 217–226. <https://doi.org/10.4067/S0717-92002018000200217>.
- Goldenberg, M.G., F.J. Oddi, J.H. Gowda, and L.A. Garibaldi. 2020. Effects of firewood harvesting intensity on biodiversity and ecosystem services in shrublands of northern Patagonia. *Forest Ecosystems* 7: 1–14. <https://doi.org/10.1186/s40663-020-00255-y>.
- Goldenberg, M.G., F.J. Oddi, J.H. Gowda, and L.A. Garibaldi. 2021. Shrubland management in northwestern Patagonia: an evaluation of its short-term effects on multiple ecosystem services. In P. L. Peri, G. Martínez Pastur and L. Nahuelhual (Eds.), *Ecosystem Services in Patagonia: A Multi-Criteria Approach for an Integrated Assessment*, 99–114. Springer, Cham, Switzerland.
- Gorelick, N., M. Hancher, M. Dixon, S. Ilyushchenko, D. Thau, and R. Moore. 2017. Google Earth Engine: Planetary-scale geospatial analysis for everyone. *Remote Sensing of Environment* 202: 18–27. <https://doi.org/10.1016/j.rse.2017.06.031>.
- Greenwell, B.M. 2017. pdp: An R Package for Constructing Partial Dependence Plots. *The R Journal* 9: 421–436.
- Hijmans, R.J., S.E. Cameron, J.L. Parra, P.G. Jones, and A. Jarvis. 2005. Very high resolution interpolated climate surfaces for global land areas. *International Journal of Climatology: A Journal of the Royal Meteorological Society* 25 (15): 1965–1978. <https://doi.org/10.1002/joc.1276>.
- Holden, Z.A., and W.M. Jolly. 2011. Modeling topographic influences on fuel moisture and fire danger in complex terrain to improve wildland fire management decision support. *Forest Ecology and Management* 262 (12): 2133–2141. <https://doi.org/10.1016/j.foreco.2011.08.002>.
- Holsinger, L., S.A. Parks, and C. Miller. 2016. Weather, fuels, and topography impede wildland fire spread in western US landscapes. *Forest Ecology and Management* 380: 59–69. <https://doi.org/10.1016/j.foreco.2016.08.035>.
- Holz, A., T. Kitzberger, J. Paritsis, and T.T. Veblen. 2012. Ecological and climatic controls of modern wildfire activity patterns across southwestern South America. *Ecosphere* 3 (11): 1–25. <https://doi.org/10.1890/ES12-00234.1>.
- Huntington, J.L., K.C. Hegewisch, B. Daudert, C.G. Morton, J.T. Abatzoglou, D.J. McEvoy, and T. Erickson. 2017. Climate Engine: Cloud computing and visualization of climate and remote sensing data for advanced natural resource monitoring and process understanding. *Bulletin of the American Meteorological Society* 98 (11): 2397–2410. <https://doi.org/10.1175/BAMS-D-15-00324.1>.
- Iniguez, J.M., T.W. Swetnam, and S.R. Yool. 2008. Topography affected landscape fire history patterns in southern Arizona, USA. *Forest Ecology and Management* 256 (3): 295–303. <https://doi.org/10.1016/j.foreco.2008.04.023>.
- Jucker, T., S.R. Hardwick, S. Both, D.M.O. Elias, R. Ewers, D.T. Milodowski, T. Swinfield, and D.A. Coomes. 2018. Canopy structure and topography jointly constrain the microclimate of human-modified tropical landscapes. *Global Change Biology* 24 (11): 5243–5258. <https://doi.org/10.1111/gcb.14415>.
- Kitzberger, T., E. Araújo, J.H. Gowda, M. Mermoz, and J.M. Morales. 2012. Decreases in fire spread probability with forest age promotes alternative community states, reduced resilience to climate variability and large fire regime shifts. *Ecosystems* 15: 97–112. <https://doi.org/10.1007/s10021-011-9494-y>.
- Kitzberger, T., G.L.W. Perry, J. Paritsis, J.H. Gowda, A.J. Tepley, A. Holz, and T.T. Veblen. 2016. Fire–vegetation feedbacks and alternative states: common mechanisms of temperate forest vulnerability to fire in southern South America and New Zealand. *New Zealand Journal of Botany* 54 (2): 247–272. <https://doi.org/10.1080/0028825X.2016.1151903>.
- Kitzberger, T., E. Raffaele, K. Heinemann, and M.J. Mazzarino. 2005. Effects of fire severity in a north Patagonian subalpine forest. *Journal of Vegetation Science* 16 (1): 5–12. <https://doi.org/10.1111/j.1654-1103.2005.tb02333.x>.
- Kitzberger, T., F. Tiribelli, I. Barberá, J.H. Gowda, J.M. Morales, L. Zalazar, and J. Paritsis. 2022. Projections of fire probability and ecosystem vulnerability under 21st century climate across a trans-Andean productivity gradient in Patagonia. *Science of the Total Environment* 839: 156303. <https://doi.org/10.1016/j.scitotenv.2022.156303>.
- Kitzberger, T., and T.T. Veblen. 1997. Influences of humans and ENSO on fire history of *Austrocedrus chilensis* woodlands in northern Patagonia. *Argentina. Ecoscience* 4 (4): 508–520. <https://doi.org/10.1080/11956860.1997.11682430>.
- Kitzberger, T., and T.T. Veblen. 2003. Influences of climate on fire in northern Patagonia, Argentina. In T. T. Veblen, W. L. Baker, G. Montenegro, T. W. Swetnam (Eds.), *Fire and climatic change in temperate ecosystems of the western Americas*, 296–321. Springer-Verlag, New York.
- Kitzberger, T., T.T. Veblen, and R. Villalba. 1997. Climatic influences on fire regimes along a rainforest-to-xeric woodland gradient in northern Patagonia. *Argentina. Journal of Biogeography* 24 (1): 35–47. <https://doi.org/10.1111/j.1365-2699.1997.tb00048.x>.
- Krawchuk, M.A., and M.A. Moritz. 2011. Constraints on global fire activity vary across a resource gradient. *Ecology* 92 (1): 121–132. <https://doi.org/10.1890/09-1843.1>.
- Krawchuk, M.A., M.A. Moritz, M.A. Parisien, J. Van Dorn, and K. Hayhoe. 2009. Global pyrogeography: the current and future distribution of wildfire. *PloS One* 4 (4): e5102. <https://doi.org/10.1371/journal.pone.0005102>.
- Landesmann, J.B., and J.M. Morales. 2018. The importance of fire refugia in the recolonization of a fire-sensitive conifer in northern Patagonia. *Plant Ecology* 219: 455–466. <https://doi.org/10.1007/s11258-018-0808-4>.
- Landesmann, J.B., F. Tiribelli, J. Paritsis, T.T. Veblen, and T. Kitzberger. 2021. Increased fire severity triggers positive feedbacks of greater vegetation flammability and favors plant community-type conversions. *Journal of Vegetation Science* 32 (1): e12936. <https://doi.org/10.1111/jvs.12936>.
- Laner, K.F., S. Waidlich, V.B. Zimmerman, and M.M. Denham. 2020. First steps towards a dynamical model for forest fire behaviour in Argentinian landscapes. *Journal of Computer Science & Technology* 20(2). <https://doi.org/10.24215/16666038.20.e09>.
- Lara, A., P. Rutherford, C. Montory, D. Bran, A. Pérez, S. Clayton, J. Ayasa, D. Barrios, M. Gross, and G. Iglesias. 1999. Vegetación de la eco-región de los bosques valdivianos. WWF. *Fundación Vida Silvestre, Boletín Técnico* 51: 1–29.
- Lizundia-Loiola, J., G. Otón, R. Ramo, and E. Chuvieco. 2020. A spatio-temporal active-fire clustering approach for global burned area mapping at 250 m from MODIS data. *Remote Sensing of Environment* 236: 111493. <https://doi.org/10.1016/j.rse.2019.111493>.
- Long, T., Z. Zhang, G. He, W. Jiao, C. Tang, B. Wu, X. Zhang, G. Wang, and R. Yin. 2019. 30 m resolution global annual burned area mapping based on

- Landsat Images and Google Earth Engine. *Remote Sensing* 11 (5): 489. <https://doi.org/10.3390/rs11050489>.
- Lund, M.T., K. Nordling, A.B. Gjelsvik, and B.H. Samset. 2023. The influence of variability on fire weather conditions in high latitude regions under present and future global warming. *Environmental Research Communications* 5 (6): 065016. <https://doi.org/10.1088/2515-7620/acdfad>.
- Marchal, J., S.G. Cumming, and E.J.B. McIntire. 2020. Turning down the heat: vegetation feedbacks limit fire regime responses to global warming. *Ecosystems* 23: 204–216. <https://doi.org/10.1007/s10021-019-00398-2>.
- Méndez-Toribio, M., J.A. Meave, I. Zermeño-Hernández, and G. Ibarra-Manríquez. 2016. Effects of slope aspect and topographic position on environmental variables, disturbance regime and tree community attributes in a seasonal tropical dry forest. *Journal of Vegetation Science* 27 (6): 1094–1103. <https://doi.org/10.1111/jvs.12455>.
- Mermoz, M. 2002. Detección y mapeo de incendios forestales en los parques nacionales de nor-Patagonia, período 1985–1999. Delegación Regional Patagonia, Administración de Parques Nacionales.
- Mermoz, M., T. Kitzberger, and T.T. Veblen. 2005. Landscape influences on occurrence and spread of wildfires in Patagonian forests and shrublands. *Ecology* 86 (10): 2705–2715. <https://doi.org/10.1890/04-1850>.
- Miller, J.D., C.N. Skinner, H.D. Safford, E.E. Knapp, and C.M. Ramirez. 2012. Trends and causes of severity, size, and number of fires in northwestern California, USA. *Ecological Applications* 22 (1): 184–203. <https://doi.org/10.1890/10-2108.1>.
- Mitchell, R.J., J.K. Hiers, J. O'Brien, and G. Starr. 2009. Ecological forestry in the Southeast: Understanding the ecology of fuels. *Journal of Forestry* 107 (8): 391–397. <https://doi.org/10.1093/jof/107.8.391>.
- Morales, J.M., M. Mermoz, J.H. Gowda, and T. Kitzberger. 2015. A stochastic fire spread model for north Patagonia based on fire occurrence maps. *Ecological Modelling* 300: 73–80. <https://doi.org/10.1016/j.ecolmodel.2015.01.004>.
- Mundo, I.A., T. Wiegand, R. Kanagaraj, and T. Kitzberger. 2013. Environmental drivers and spatial dependency in wildfire ignition patterns of north-western Patagonia. *Journal of Environmental Management* 123: 77–87. <https://doi.org/10.1016/j.jenvman.2013.03.011>.
- Oddi, F.J., and L. Ghermandi. 2016. Fire regime from 1973 to 2011 in north-western Patagonian grasslands. *International Journal of Wildland Fire* 25 (9): 922–932. <https://doi.org/10.1071/WF15211>.
- OpenStreetMap Contributors. 2015. Retrieved from <http://www.openstreetmap.org/>. Accessed Dec 2018.
- Oyarzabal, M., J. Clavijo, L. Oakley, F. Biganzoli, P. Tognetti, I. Barberis, H.M. Maturo, et al. 2018. Vegetation units of Argentina. *Ecología Austral* 28 (01): 040–063. <https://doi.org/10.25260/EA.18.28.1.0.399>.
- Paritsis, J., A. Holz, T.T. Veblen, and T. Kitzberger. 2013. Habitat distribution modeling reveals vegetation flammability and land use as drivers of wildfire in SW Patagonia. *Ecosphere* 4 (5): 1–20. <https://doi.org/10.1890/ES12-00378.1>.
- Paritsis, J., T.T. Veblen, and A. Holz. 2015. Positive fire feedbacks contribute to shifts from *nothofagus pumilio* forests to fire-prone shrublands in Patagonia. *Journal of Vegetation Science* 26 (1): 89–101. <https://doi.org/10.1111/jvs.12225>.
- Pausas, J.G., and E. Ribeiro. 2013. The global fire–productivity relationship. *Global Ecology and Biogeography* 22 (6): 728–736. <https://doi.org/10.1111/geb.12043>.
- Peri, P.L., H.A. Bahamonde, M.V. Lencinas, V. Gargaglione, R. Soler, S. Ormaechea, and G. Martínez Pastur. 2016. A review of silvopastoral systems in native forests of *Nothofagus antarctica* in southern Patagonia, Argentina. *Agroforestry Systems* 90: 933–960. <https://doi.org/10.1007/s10457-016-9890-6>.
- Pricope, N.G., and M.W. Binford. 2012. A spatio-temporal analysis of fire recurrence and extent for semi-arid savanna ecosystems in southern Africa using moderate-resolution satellite imagery. *Journal of Environmental Management* 100: 72–85. <https://doi.org/10.1016/j.jenvman.2012.01.024>.
- Pueyo, S., P.M.L. de Alencastro Graça, R. Imbrozio Barbosa, R. Cots, E. Cardona, and P.M. Fearnside. 2010. Testing for criticality in ecosystem dynamics: The case of Amazonian rainforest and savanna fire. *Ecology Letters* 13 (7): 793–802. <https://doi.org/10.1111/j.1461-0248.2010.01497.x>.
- Pyra, N. 2024. scam: Shape Constrained Additive Models. R package version 1.2–13. <https://CRAN.R-project.org/package=scam>.
- R Core Team. 2022. R: a language and environment for statistical computing. Vienna, Austria: R Foundation for Statistical Computing. <https://www.R-project.org/>.
- Riddle, A.A. 2023. Wildfire Statistics. Congressional Research Service. <https://crsreports.congress.gov/product/pdf/IF/IF10244>.
- Robinne, F.N., J. Burns, P. Kant, M. Flannigan, M. Kleine, B. de Groot, and D.M. Wotton. 2018. Global fire challenges in a warming world. In *Proceedings of the Global Expert Workshop on Fire and Climate Change*, eds. Robinne, F.N., J. Burns, P. Kant, M. Flannigan, M. Kleine, B. de Groot, and D.M. Wotton, 1–32. Vienna: International Union of Forest Research Organizations (IUFRO); <https://www.iufro.org/publications/series/occasional-papers/article/2018/01/01/op32-global-fire-challenges-in-a-warming-world/>.
- Rothermel, R.C. 1983. How to Predict the Spread and Intensity of Forest and Range Fires. Ogden: U.S. Department of Agriculture, Forest Service, Intermountain Forest and Range Experiment Station; https://www.fs.usda.gov/rm/pubs_int/int_gtr143.pdf.
- Ryan, K.C., E.E. Knapp, and J.M. Varner. 2013. Prescribed fire in North American forests and woodlands: History, current practice, and challenges. *Frontiers in Ecology and the Environment* 11 (s1): e15–24. <https://doi.org/10.1890/120329>.
- Seidl, R., J. Honkaniemi, T. Aakala, A. Aleinikov, P. Angelstam, M. Bouchard, Y. Boulanger, et al. 2020. Globally consistent climate sensitivity of natural disturbances across boreal and temperate forest ecosystems. *Ecography* 43 (7): 967–978. <https://doi.org/10.1111/ecog.04995>.
- Shuman, J.K., J.K. Balch, R.T. Barnes, P.E. Higuera, C.I. Roos, D.W. Schwilk, E.N. Stavros, et al. 2022. Reimagine fire science for the Anthropocene. *PNAS Nexus* 1 (3): pgac115. <https://doi.org/10.1093/pnasnexus/pgac115>.
- Simon, A., J. Fierke, E.J. Reiter, G.A. Loguercio, S. Heinrichs, B. Putzenlechner, N.Z. Joelson, and H. Walentowski. 2024. The interior climate and its microclimatic variation of temperate forests in northern Patagonia, Argentina. *International Journal of Biometeorology*, 1–12. <https://doi.org/10.1007/s00484-024-02617-5>.
- Sommerfeld, A., C. Senf, B. Buma, A.W. D'Amato, T. Després, I. Díaz-Hormazábal, S. Fraver, et al. 2018. Patterns and drivers of recent disturbances across the temperate forest biome. *Nature Communications* 9 (1): 4355. <https://doi.org/10.1038/s41467-018-06788-9>.
- Tercero-Bucardo, N., T. Kitzberger, T.T. Veblen, and E. Raffaele. 2007. A field experiment on climatic and herbivore impacts on post-fire tree regeneration in north-western Patagonia. *Journal of Ecology* 95 (4): 771–779. <https://doi.org/10.1111/j.1365-2745.2007.01249.x>.
- Thompson, D.W.J., S. Solomon, P.J. Kushner, M.H. England, K.M. Grise, and D.J. Karoly. 2011. Signatures of the antarctic ozone hole in Southern Hemisphere surface climate change. *Nature Geoscience* 4 (11): 741–749. <https://doi.org/10.1038/ngeo1296>.
- Tian, X., D.J. McRae, J. Jin, L. Shu, F. Zhao, and M. Wang. 2011. Wildfires and the Canadian Forest Fire Weather Index system for the Daxing'anling region of China. *International Journal of Wildland Fire* 20 (8): 963–973. <https://doi.org/10.1071/WF09120>.
- Tiribelli, F., T. Kitzberger, and J.M. Morales. 2018. Changes in vegetation structure and fuel characteristics along post-fire succession promote alternative stable states and positive fire–vegetation feedbacks. *Journal of Vegetation Science* 29 (2): 147–156. <https://doi.org/10.1111/jvs.12620>.
- Tiribelli, F., J.M. Morales, J.H. Gowda, M. Mermoz, and T. Kitzberger. 2019. Non-additive effects of alternative stable states on landscape flammability in NW Patagonia: Fire history and simulation modelling evidence. *International Journal of Wildland Fire* 28 (2): 149–159. <https://doi.org/10.1071/WF18073>.
- De Torres Curth, M.J., L. Ghermandi, and G. Pfister. 2008. Los incendios en el noroeste de la Patagonia: Su relación con las condiciones meteorológicas y la presión antrópica a lo largo de 20 años. *Ecología Austral* 18 (2): 153–167.
- Veblen, T.T., T. Kitzberger, E. Raffaele, M. Mermoz, M.E. González, J.S. Sibold, and A. Holz. 2008. The historical range of variability of fires in the Andean-Patagonian *Nothofagus* forest region. *International Journal of Wildland Fire* 17 (6): 724–741. <https://doi.org/10.1071/WF07152>.
- Villagra, P.E., E. Cesca, L.M. Alvarez, S. Delgado, and R. Villalba. 2024. Spatial and temporal patterns of forest fires in the Central Monte: Relationships with regional climate. *Ecological Processes* 13 (1): 5. <https://doi.org/10.1186/s13717-023-00481-6>.
- Villalba, R., A. Lara, J.A. Boninsegna, M. Masiokas, S. Delgado, J.C. Aravena, F.A. Roig, A. Schmelter, A. Wolodarsky, and A. Ripalta. 2003. Large-scale temperature changes across the Southern Andes: 20th-century variations

- in the context of the past 400 years. *Climatic Change* 59 (1): 177–232. <https://doi.org/10.1023/A:1024452701153>.
- Vitolo, C., F. Di Giuseppe, C. Barnard, R. Coughlan, J. San-Miguel-Ayanz, G. Libertá, and B. Krzeminski. 2020. ERA5-based global meteorological wildfire danger maps. *Scientific Data* 7 (1): 216. <https://doi.org/10.1038/s41597-020-0554-z>.
- van Wagner, C.E. 1987. Development and Structure of the Canadian Forest Fire Weather Index System. *Forestry Technical Report* (35). Ottawa: Canadian Forestry Service. https://publications.gc.ca/collections/collection_2018/mcan-nrcan/Fo29-2/Fo29-2-43-1987-eng.pdf.
- Wang, X., D.K. Thompson, G.A. Marshall, C. Tymstra, R. Carr, and M.D. Flannigan. 2015. Increasing frequency of extreme fire weather in Canada with climate change. *Climatic Change* 130: 573–586. <https://doi.org/10.1007/s10584-015-1375-5>.
- Whitlock, C., D.B. McWethy, A.J. Tepley, T.T. Veblen, A. Holz, M.S. McGlone, G.L.W. Perry, J.M. Wilmshurst, and S.M. Wood. 2015. Past and present vulnerability of closed-canopy temperate forests to altered fire regimes: A comparison of the Pacific Northwest, New Zealand, and Patagonia. *BioScience* 65 (2): 151–163. <https://doi.org/10.1093/biosci/biu194>.
- Wood, S.M., B.P. Murphy, and D.M.J.S. Bowman. 2011. Firescape Ecology: How topography determines the contrasting distribution of fire and rain forest in the south-west of the Tasmanian Wilderness World Heritage Area. *Journal of Biogeography* 38 (9): 1807–1820. <https://doi.org/10.1111/j.1365-2699.2011.02524.x>.
- Wood, S. 2017. Generalized Additive Models: An Introduction with R (2nd ed.). Boca Raton: Chapman and hall/CRC.
- Woodward, F.I., and I.F. McKee. 1991. Vegetation and climate. *Environment International* 17 (6): 535–546. [https://doi.org/10.1016/0160-4120\(91\)90166-N](https://doi.org/10.1016/0160-4120(91)90166-N).

Publisher's Note

Springer Nature remains neutral with regard to jurisdictional claims in published maps and institutional affiliations.